

Tomographische Untersuchungen magnetischer CVs mit HST und ROSAT

Schlussbericht zum Vorhaben FKZ 50 OR 9706 8

1 Aufgabenstellung und Voraussetzungen

1.1 Aufgabenstellung

Das Vorhaben ‘Tomographische Untersuchungen magnetischer CVs mit HST’ (1997 – 1999) und daran anknüpfend ‘... mit HST und ROSAT’ (1999 – 2002) hatte zum Ziel, umfangreiches mit ROSAT im Gastbeobachterprogramm eingeworbenes Datenmaterial magnetischer CVs systematisch zu untersuchen. Besonderes Augenmerk lag hier auf dem hellsten, bedeckenden dieser Sternsysteme, HU Aqr, für das auch umfangreiche HST-Beobachtungen und weitere Beobachtungen im optischen Spektralbereich eingeworben wurden. Es sollten die Eigenschaften des Akkretionsstroms, des Akkretionsvorhanges, der Akkretionsregion auf dem Weissen Zwerg, sowie die Parameter des Masse abgebenden Begleitsterns entschlüsselt werden. Im Rahmen verschiedener Identifikationsprogramme heller Quellen des ROSAT all-sky survey wurden diverse neue CVs identifiziert. Die Eigenschaften der CVs als Gruppe nach Abschluss der ROSAT Himmelsdurchmusterung sollte charakterisiert werden.

1.2 Voraussetzungen

Ein Hauptaugenmerk dieses Projekts lag auf dem hellsten dieser Sternsysteme, das eine Sternbedeckung zeigt, HU Aqr. Von diesem System wurden 200 ksec mit dem ROSAT-PSPC und dem HRI, sowie ergänzend eine halbe Mega-Sekunde mit dem amerikanischen Satelliten EUVE gewonnen, die im Rahmen des Vorhabens analysiert wurden. Des weiteren wurde dieses System mit dem Hubble Space Telescope HST in insgesamt 12 Orbits mit spektral hoher und niedriger Auflösung beobachtet. Ergänzend wurde optisch bodengebundene Spektroskopie und Hochgeschwindigkeitsphotometrie durchgeführt. Um die an HU Aqr erzielten Ergebnisse auf ihre Relevanz, sprich allgemeinere Gültigkeit zu testen, wurden weitere bedeckende Systeme mit HST, ROSAT, und mit bodengebundenen Teleskopen, detailliert beobachtet.

2 Durchführung

2.1 Tomographische Untersuchungen magnetischer CVs

Röntgentomographie mit ROSAT und EUVE

Mit Hilfe der detaillierten ROSAT-Beobachtungen von HU Aqr sollte die Dichteverteilung in Akkretionsströmen und -schleiern bestimmt werden, um daraus Rückschlüsse auf die Magnetosphärenphysik (Ankoppelung des Stromes ans Magnetfeld) zu ziehen.

Es sollte die dreidimensionale Struktur der Akkretionsregionen (zumindest näherungsweise) erschlossen werden durch eine Entfaltung der Röntgenlichtkurve unter Zuhilfenahme der Einschränkungen, die aus Bedeckungen und Selbstbedeckungen abgeleitet werden können. Dies erlaubt Rückschlüsse auf die Physik der Umwandlung von Gravitationsenergie in Strahlung.

Eclipse mapping mit ROSAT, HST, und XMM-Newton

Mit Hilfe von ROSAT-Beobachtungen sollten Einschränkungen an die Größe der weiche Röntgenstrahlung emittierenden Region abgeleitet werden, mit HST die Entsprechung im Ultraviolett-Bereich. Die Ungleichzeitigkeit der bislang vorliegenden Beobachtungen erschwert wegen der immanenten hohen Variabilität der Quellen die eindeutige Interpretation. Besonders große Bedeutung liegt deshalb auf der Vorbereitung von Beobachtungen mit XMM-Newton, das gleichzeitig Beobachtungen im weichen und harten Röntgenbereich und im Ultraviolett-Bereich erlaubt.

In den durch die masseabgebenden Begleitsterne hervorgerufenen Bedeckungen der Weißen Zwerge sollte nach koronaler Röntgenemission vom Sekundärstern und nach Röntgenemission vom Akkretionsstrom gesucht werden, letzteres durch dissipative Prozesse beim Einfangen des Stromes vom Magnetfeld hervorgerufen.

Es war geplant, die satellitenbestützten Beobachtungen jeweils durch detaillierte optische Beobachtungen zu unterstützen.

Mapping des heißen Flecks mit HST

Es sollte ein parametrisiertes Modell der UV-Emission entwickelt werden, das an phasenaufgelöste, mit hoher Zeitaufösung gewonnene Beobachtungsdaten angepaßt wird. In einem zweiten Schritt sollte durch genetische Algorithmen Temperaturkarten des Akkretionsflecks berechnet werden. Ziel dieser Untersuchungen ist die Bestimmung der Parameter (Größe, Temperatur) der UV-Flecken in den Akkretionsregionen der Weißen Zwerge. Daraus können Rückschlüsse auf die Reprozessierung der Röntgenstrahlung gezogen werden.

Dopplertomographie mit Emissions- und Absorptionslinien im UV, Optischen und Nahinfrarot

Verschiedene Ansätze zum Verständnis der komplexen Linienstrukturen wurden im Rahmen des Projektes verfolgt. Zur Interpretation der mit MEM-Verfahren abgeleiteten Dopplertomogramme wurden zunächst einfache Trajektorienmodelle, später auch darauf aufbauend simulierte getraillte Spektrogramme erstellt.

Es wurde ein Modell des ram-pressure stripping entwickelt, mit dem getraillte Spektrogramme und Dopplerkarten simuliert werden konnten.

Ein anderer Ansatz stellt das in diesem Projekt entwickelte accretion stream mapping dar. Dabei wird die gemessene Linienlichtkurve auf den Akkretionsstrom oder -schleier abgebildet. Dieses Verfahren liefert komplementäre Information über den Helligkeitsverlauf entlang des Akkretionsstromes und damit über die Anregungsbedingungen.

Durch Dopplertomographie photosphärischer Absorptionslinien vom Begleitstern (insbesondere Na $\lambda\lambda 8183/8194$) wurde die Bedeutung der Röntgenheizung für die Atmosphären der Begleiter erkannt. Die Technik der Roche-Tomographie wurde begleitend zu diesem Projekt in derselben Arbeitsgruppe entwickelt und erlaubt die direkte Vermessung der Größe der Begleitsterne im Geschwindigkeitsraum und die Suche nach Sternflecken auf diesen Spättypsternen.

2.2 Neue mCVs aus der ROSAT-Himmelsdurchmusterung

Die mit ROSAT neu gefundenen und im ROSAT Bright Survey als solche identifizierten CVs sollten als Gruppe studiert und optisch nachbeobachtet werden, um wesentliche Parameter dieser Systeme festzulegen. Dazu gehören die Feststellung des Subtyps, die Bestimmung der Entfernung und der Bahnumlafperiode, die entweder aus photometrischen oder spektroskopischen Beobachtungen erschlossen werden können.

3 Zusammenarbeit mit anderen Stellen

- Max-Planck Institut für Extraterrestrische Physik: ROSAT Survey (W. Voges), Hochgeschwindigkeitsphotometrie (Kanbach)
- Center for EUVE astrophysics: EUVE-Beobachtungen (M. Sirk)
- Universitäts-Sternwarte Göttingen: Optische Identifikationen (Beuermann, Reinsch)
- South African Astronomical Observatory: Accretion Stream Mapping (Vriellmann)
- Universität St. Andrews: Doppler-Tomographie, HST-Beobachtungen (Horne)
- Max-Planck-Institut für Astrophysik: Optische Identifikationen (Thomas)

- University Southampton: Hochgeschwindigkeitsphotometrie (Marsh), Spot mapping, HST-Beobachtungen (Gänsicke)
- Universitäts-Sternwarte München: Hochgeschwindigkeitsphotometrie (Barwig, Mantel)
- Leicester University: XMM-Beobachtungen (Osborne, Wheatley)

4 Mitarbeiter im Projekt

Mitarbeiter	Status	G/P	Laufzeit
G. Hasinger	Projektleitung	G	bis 03.99
A. Schwope	post-doc	G	ab 03.99
A. Schwope	Projektleitung	G	ab 03.99
R. Schwarz	Doktorand	P	1.4.1997 – 30.4.2002
V. Hambaryan	Post-doc	P	15.8.1999 – 30.4.2002
A. Staude	Doktorand	G	05.99 – 30.4.2002
D. Meinert	EDV	G	
K.-H. Boening	EDV	G	

5 Ergebnisse

5.1 Wissenschaftliche Ergebnisse

Es wurde ein Modell für die UV-Emission des heißen Flecks auf HU Aqr anhand von HST-Daten erstellt. Es beinhaltet eine detaillierte Bedeckungsgeometrie und wahlweise eine lineare, gaussförmige oder exponentielle Temperaturstruktur. Die Beobachtungsdaten lassen eine Unterscheidung der möglichen Temperaturstrukturmodelle nicht zu. Das gleiche Modell wurde mit Erfolg auch auf die HST-Daten von V1309 Ori, DP Leo und UZ For angewandt. Es zeigt sich, dass bedeckende Sternsysteme von ganz entscheidender Bedeutung sind, um die Entartung der Parameter Entfernung, Größe des Weißen Zwerges, und Größe des heißen Flecks aufzuheben. Die ist in diesem Projekt erstmals gelungen und wird im Anschluss mit XMM-Newton fortgesetzt (Röntgenteleskop und optischer Monitor).

Detaillierte Analysen der beiden hellsten bedeckenden AM Herculis Sterne UZ For und HU Aqr mit ROSAT wurden durchgeführt, entsprechende Daten mit XMM-Newton wurden nach Abschluss des Vorhabens aufgenommen. Im Vorhaben wurden jedoch die Grundlagen für die erfolgreiche Antragstellung und Bearbeitung der XMM-Daten gelegt. Die ROSAT Analysen haben es erlaubt, erstmals die Struktur eines Röntgenakkretionsflecks in drei Dimensionen aufzulösen. Es zeigt sich, dass die Akkretionsflecken mit einem Durchmesser von etwa 500 km sehr kompakt sind. Detaillierte Beobachtungen mit hoher Zeitauflösung bei verschiedenen Wellenlängen (optisch, UV, X) zeigen die unterschiedlichen Größen der verschiedenen Emissionsgebiete und geben direkte Hinweise auf einen räumlichen Versatz des Zyklotronstrahlung aussendenden Hochtemperaturplasmas (5–10 keV) vom wesentlich kühleren Akkretionsfleck, der das ROSAT und EUVE-Band beherrscht. Die aus Zyklotronbeobachtungen vorhergesagte räumlich weit ausgedehnte harte Röntgenkomponente kann nur mit XMM-Beobachtungen nachgewiesen werden.

Es wurden die weltweit besten und aussagekräftigsten Dopplertomogramme einer ganzen Reihe von AM Herculis Sternen gewonnen. Die darin typischerweise erkennbaren Strukturen können dem röntgenbestrahlten Sekundärstern, dem ballistischen Strom und dem magnetisch dominierten Strom zugeordnet werden. Wenn auch ein prinzipielles Verständnis der komplexen Emissionslinienspektren der AM Herculis Sterne erzielt wurde, wurden im Rahmen dieses Projektes jedoch auch sehr große Abweichungen der beobachteten Tomogramme gegenüber den relativ einfachen Modellvorstellungen festgestellt. So sind die Bestrahlungseffekte der Sekundärsterne i.A. nicht symmetrisch, was auf die weitverbreitete Anwesenheit sog. Akkretionsschleier hinweist, die anderweitig nicht nachweisbar sind. Desweiteren sind die ballistischen Ströme in Realität wahrscheinlich alles andere als ballistisch, sondern in großen Teilen gleich von Beginn am Begleitstern (am L_1 oder an anderen Stellen) dominiert oder stark beeinflusst durch die im Doppelsystem herrschenden Magnetfelder. Eine wesentlich Rolle scheint dabei auch das bislang unterschätzte Magnetfeld des Begleitsterns zu spielen. Die Teile des Akkretionsstromes, die ganz eindeutig durch das Magnetfeld dominiert werden, zeigen eine sehr große Vielfalt in ihrer Struktur, die einerseits durch die

unterschiedlichen Akkretionsgeometrien der verschiedenen Systeme, andererseits durch wechselnde Akkretionsraten bedingt sind.

Es wurde ein quantitatives Modell der Emissionslinien aus dem Akkretionsstrom erarbeitet und mit den Beobachtungen von HU Aqr in einem leuchtkräftigen Zustand verglichen. Es hat gute Aussagekraft in bezug auf die Akkretionsgeometrie, die Massenakkretionsrate, und die Orientierung des Magnetfeldes im Sternsystem. Ein sehr detailliertes Verständnis der beobachteten Linienbreiten steht allerdings noch aus.

Dopplertomographie des asynchron rotierenden Polars BY Cam zeigt deutliche Unterschiede der Stromemission im Vergleich zu synchron rotierenden AM Herculis-Sternen. Es konnte nachgewiesen werden, daß ein Teil der Materie weit um den Weißen Zwerg herumläuft und nicht zum energetisch bevorzugten Pol geführt wird.

Es wurde ein Programmcode zum Accretion Stream Mapping entwickelt und erfolgreich auf HU Aqr in einem leuchtkräftigen Zustand angewandt. Diese Daten legen eine erhöhte Leuchtkraft des Akkretionsstromes in der Wechselwirkungsregion zwischen Strom und Magnetfeld nahe. Diese Ergebnisse sind jedoch noch nicht eindeutig und benötigen zur Bestätigung hochaufgelöste Spektroskopie mit sehr hoher Zeitauflösung, eine Aufgabe für Teleskope der 10m-Klasse.

Mit Hilfe der Roche Tomographie war es erstmals möglich, die Größe eines Begleitsterns in einem Polar im Geschwindigkeitsraum aufzulösen. Die Methoden und Ergebnisse sind vielversprechend, um mit künftigen Daten, die an größeren Teleskopen gewonnen werden sollen, erfolgreich nach Sternflecken suchen zu können.

Ein Visualisierungsprogramm der Strom- und Bedeckungsgeometrien der AM Herculis Sterne wurde entwickelt, ein sehr hilfreiches Werkzeug zum Verständnis der Bedeckungsvorgänge.

In einer den ROSAT Bright Survey RBS (Identifikation der 2000 hellsten ROSAT-Quellen bei hohen galaktischen Breiten, PI Schwobe) abschliessenden Publikation wurden die kombinierten Röntgenoptischen Eigenschaften der RBS-CVs beschrieben und eine neue Schätzung der Raumdicke abgeleitet. In diesem Programm wurden die ersten beiden CVs, die eine Eigenbewegung zeigen und daher nah sein müssen, detektiert. Sollte sich die erste vorsichtige Schätzung von 30 pc von RBS0490 und RBS1955 bestätigen, könnte die Raumdicke der nichtmagnetischen CVs um einen Faktor 10 höher liegen als bislang angenommen. Folgebeobachtungen sind absolut notwendig und wurden initiiert.

5.2 Wirtschaftliche Erfolgsaussichten

Das Vorhaben liegt im Bereich der astrophysikalischen Grundlagenforschung. Es wurden Satellitendaten, die mit HST, ROSAT, EUVE, und XMM-Newton gewonnen wurden, sowie unterstützende bodengebundene optische Beobachtungsdaten ausgewertet.

Unmittelbare wirtschaftliche Erfolgsaussichten bestehen daher im engen Sinne im Rahmen des beantragten Projekts nicht, da nicht gezielt Produkte für einen bereits bestehenden oder zu erschließenden Markt entwickelt werden. Das akkumulierte und entwickelte know-how ist jedoch in zweierlei Hinsicht von Bedeutung für den Wirtschaftsstandort Deutschland. Zum einen fließen die erworbenen Kenntnisse und das erworbene Verständnis zurück in die Entwicklung und Optimierung zukünftiger Satellitenmissionen. Zum anderen qualifiziert der Umgang mit und die Entwicklung von modernen Bildverarbeitungs-, Optimierungs- und Analyse-Codes die auf diesem Projekt Angestellten zu vielfältiger Tätigkeit auf dem wissenschaftlich-technischen Arbeitsmarkt. Tomographische Untersuchungsmethoden sind beispielsweise relevant in der medizinischen Diagnostik, aus der die in diesem Projekt benutzten Verfahren ursprünglich entlehnt wurden, und in der Materialforschung, insbesondere in der zerstörungsfreien Werkstoffprüfung.

5.3 Wissenschaftliche/technische Verwertung

Die wissenschaftlichen Ergebnisse des Projektes wurden genutzt, um der deutschen Astronomie in der weltweiten astro-community Geltung zu verschaffen. Dies geschah durch persönliche Kontakte, durch viele Publikationen, durch Konferenzvorträge, und auch durch populärwissenschaftliche Vorträge, in der der deutsche Steuerzahler direkt über die Arbeit der von ihm ausgehaltenen Wissenschaftler informiert wurde. Studenten, Schüler und Praktikanten haben im Projekt oder nahe zum Projekt gearbeitet und konnten sich so ein eigenes Bild von wissenschaftlicher Arbeit machen.

Es ist ein reicher Datenfundus zur Bearbeitung angelegt und ausgewertet worden (betrifft die instrumentelle Seite des Vorhabens) und komplexe Analysesoftware ist entwickelt worden.

Eine wichtige Rolle dabei spielt der weitere Ausbau der nationalen und internationalen Zusammenarbeit, die in den Vorjahren begonnen und erfolgreich gestaltet wurde. Zeugnis davon legt die gemeinsame Publikationstätigkeit mit auf verwandtem Gebiet arbeitenden Wissenschaftlern in Deutschland (MPA Garching, Univ. Göttingen), England (Univ. Keele, Univ. St. Andrews) und Südafrika (SAAO, Univ. Cape Town) ab. Unter den an tomographischen Untersuchungen interessierten Gruppen hat sich nahezu weltweit eine gesunde Balance zwischen Wettbewerb und Kooperation herausgebildet.

5.4 Wissenschaftliche und wirtschaftliche Anschlussfähigkeit

Zunächst sei im engerem Rahmen dieses Vorhabens hervorgehoben, dass sich die am Projekt beteiligten Wissenschaftler die Voraussetzungen erarbeitet haben, um qualifizierte Beobachtungsvorschläge für die im Orbit befindlichen Grossobservatorien XMM-Newton und Chandra einzureichen und damit zunächst die wissenschaftliche Konkurrenzfähigkeit erhalten. Ein guter Schritt in diese Richtung ist mit der Beteiligung des AIP (incl. des Projektleiters) am XMM SCC (Survey Science Consortium) getan worden, wodurch Daten in garantierter Beobachtungszeit gewonnen werden.

In einem weiter gesteckten Rahmen gilt, dass die Nutzung der national geförderten Projekte der Weltraumforschung und Satellitenastronomie neben der wissenschaftlichen auch die technologische Konkurrenzfähigkeit und Attraktivität bei der Mitwirkung zukünftiger Raumfahrtprojekte für Deutschland erhält. Wegen des zunächst rein wissenschaftlichen Hintergrundes dieses Vorhabens sei hinzugefügt, insbesondere auch ausschliesslich der Grundlagenforschung dienender Raumfahrtprojekte.

Darüberhinaus bietet die hinreichende Förderung der Nutzung wissenschaftlicher Satelliten, deren Bau mit Bundesmitteln in bedeutender Höhe gefördert wurde, die Chance, dem akut drohenden Nachwuchskräfte-mangel auf wissenschaftlich-technologischem Gebiet zu begegnen.

6 Relevante Publikationen (1997 – 2003)

6.1 Publikationen in referierten Zeitschriften

1. Schwobe A.D., Beuermann K.: 1997, Cyclotron spectroscopy of VV Puppis. *Astron. Nachr.* 318(2), 111
2. Schwobe A.D., Mengel S.: 1997, Phase-resolved spectroscopy and photometry of the eclipsing polar EP Draconis (=H1907+690). *Astron. Nachr.* 318(1), 25
3. Schwobe A.D., Mantel K.-H., Horne K.: 1997, Phase-resolved high-resolution spectrophotometry of the eclipsing polar HU Aquarii. *Astron. & Astrophys.* 319, 894
4. Schwobe A.D., Mengel S., Beuermann K.: 1997, On the mass of the white dwarf in UZ Fornacis. *Astron. Astrophys.* 320, 181
5. Schwobe A.D., Buckley D.A.H., O'Donoghue D., Hasinger G., Trümper J., Voges W.: 1997, RX J2115.7–5840: a short-period, asynchronous polar. *Astron. Astrophys.* 326, 195
6. Puchnarewicz E.M., Mason K.O., Carrera F.J., Brandt W.N., Cabrera-Guerra F., Carballo R., Hasinger G., McMahon R., Mittaz J.P.D., Page M.J., Perez-Fournon I., Schwobe A.: 1997, Optical and X-ray properties of the RIXOS AGN – II. Emission lines. *MNRAS* 291, 177
7. Hasinger G., Fischer J.-U., Schwobe A.D., Boller T., Trümper J., Voges W.: 1997, Interacting galaxies – the X-ray view. *Astron. Nachr.* 318(6), 329
8. Hambaryan, V. V., L. V. Mirzoyan, R. Wichmann, J. Krautter, and R. Neuhäuser: 1997. ROSAT observations of Pleiades flare stars. *Astrophysics* 40, 354-362.
9. Abrahamyan, H. V., K. S. Gigoyan, V. V. Hambaryan, and M. Azzopardi: 1997. First Byurakan spectral sky survey. Stars of late spectral types. IX. $-15deg < \delta < -11deg$ belt. *Astrophysics* 40, 131-139.
10. Greiner, J., R. Schwarz, J. Englhauser, P. J. Groot, and T. J. Galama: 1997 GRB 970828. *IAU Circ* 6757, 1.

11. Richter, G. A., P. Kroll, J. Greiner, W. Wenzel, R. Luthardt, and R. Schwarz: 1997. S 10932 Comae - a jumping jack among the cataclysmic variables.. A&A 325, 994-1000.
12. Burwitz V., Reinsch K., Schwope A.D., Hakala P.J., Beuermann K., Rousseau T., Thomas H.-C., Gänsicke B.T., Piirola V., Vilhu O.: 1997, A new ROSAT discovered polar near the lower period limit: RX J1015.5+0904 in Leo. Astron. Astrophys. 331, 262
13. Thomas H.-C., Beuermann K., Reinsch K., Schwope A.D., Trümper J., Voges W., 1998, Identification of soft high galactic latitude RASS X-ray sources, I. A complete count-rate limited sample. Astron. Astrophys. 335, 467–478
14. Schwarz R., Schwope A.D., Beuermann K., et al.: 1998, The new long-period AM Herculis system RX J0203.8+2959. Astron. Astrophys. 338, 465
15. Gigoyan, K. S., V. V. Hambaryan, and M. Azzopardi 1998. First Byurakan spectral sky survey. Stars of late spectral types. $-11deg < \delta < -7$ deg belt. Astrophysics 41, 356-366.
16. Mirzoyan, L. V., G. N. Salukvadze, V. V. Hambaryan, and G. S. Javakhishvily 1998. Trapezium type multiple stars-instable systems.. Astrophysics 41, 59-64.
17. Greiner, J. and R. Schwarz: 1998. RX J1016.9-4103: a new soft X-ray polar in the period gap. A&A 340, 129-134.
18. Groot, P. J. and 24 colleagues 1998. A Search for Optical Afterglow from GRB 970828. ApJL 493, L27.
19. Greiner, J., R. Schwarz, and W. Wenzel 1998. Discovery of the high-field polar RX J1724.0+4114. MNRAS 296, 437-441.
20. Fischer J.-U., Hasinger G., Schwope A.D., Brunner H., Trümper J., Voges W.: 1998, The ROSAT bright survey I. Identification of an AGN sample with hard X-ray spectra. Astron. Nachr. 319 (6), 347
21. Schwope A.D., Hasinger G., Schwarz R., Haberl F., Schmidt M.: 1999, The isolated neutron star candidate RBS1223 (1RX J130848.6+212708). Astron. Astrophys. 341, L51
22. Heerlein C., Horne K., Schwope A.D.: 1999, Modelling of the magnetic accretion flow in the polar HU Aqr. MNRAS 304, 145
23. Campbell C.G., Schwope A.D.: 1999, Asynchronous rotation in the polars. Astron. Astrophys. 343, 132
24. Beuermann, K., Thomas, H.-C., Reinsch, K., Schwope A.D., Trümper, J., Voges W.: 1999, Identification of soft high galactic latitude RASS X-ray sources II. Sources with PSPC count rate $CR < 0.5$ cts/s. Astron. Astrophys. 347, 47
25. Schwope A.D., Schwarz R., Greiner J.: 1999, Zeeman lines and a single cyclotron line in the low-accretion rate polar 1RXS J012851.9–233931 (RBS0206). Astron. Astrophys. 348, 861
26. Catalán M.S, Schwope A.D., Smith R.C.: 1999, Mapping the secondary star in QQ Vulpeculae. MNRAS 310, 123
27. Motch C., Haberl F., Zickgraf F.-J., Hasinger G., Schwope A.D.: 1999, The isolated neutron star candidate RXJ J1605.3+3249. Astron. Astrophys. 351, 177
28. Hambaryan, V., R. Neuhäuser, and B. Stelzer 1999. Bayesian flare event detection. ROSAT X-ray observations of the UV Cetus type star G 131-026. A&A 345, 121-126.
29. Neuhäuser, R. and V. Hambaryan 1999. T associations in X-rays. Astrophysics 42, 234-244.
30. Thomas H.-C., Beuermann K., Burwitz V., Reinsch K., Schwope A.D.: 2000, RX J1313.2-3259, a long-period Polar discovered with ROSAT. Astron. Astrophys. 353, 646

31. Stelzer, B., R. Neuhäuser, and V. Hambaryan 2000. X-ray flares on zero-age- and pre-main sequence stars in Taurus-Auriga-Perseus. *A&A* 356, 949-971.
32. Hearty, T., R. Neuhäuser, B. Stelzer, M. Fernández, J. M. Alcalá, E. Covino, and V. Hambaryan 2000. ROSAT PSPC observations of T Tauri stars in MBM12 PSPC observations of T Tauri stars in MBM12. *A&A* 353, 1044-1054.
33. Greiner, J., D. H. Hartmann, W. Voges, T. Boller, R. Schwarz, and S. V. Zharikov: 2000. Search for GRB X-ray afterglows in the ROSAT all-sky survey. *A&A* 353, 998-1008.
34. Greiner, J., R. Schwarz, S. Zharikov, and M. Orío: 2000. RX J1420.4+5334 - another tidal disruption event? *A&A* 362, L25-L28.
35. Greiner, J., M. Orío, and R. Schwarz: 2000. RX J0537.7-7034: The shortest-period supersoft X-ray source. *A&A* 355, 1041-1048.
36. Greiner, J., G. Tovmassian, M. Orío, H. Lehmann, V. Chavushyan, A. Rau, R. Schwarz, R. Casalegno, and R.-D. Scholz: 2001. BZ Camelopardalis during its 1999/2000 optical low state. *A&A* 376, 1031-1038.
37. Schwöpe A.D., Hasinger G., Lehmann I., Schwarz R., Brunner H., Neizvestny S., Ugryumov A., Balega Yu., Trümper J., Voges W.: 2000 The ROSAT Bright Survey: II. Catalogue of all high-galactic latitude RASS sources with PSPC countrate $CR > 0.2 \text{ s}^{-1}$. *Astron. Nachr.* 321, 1
38. Mason K.O., Carrera F.J., Hasinger G., ... Schwöpe A.D. ...: 2000, The ROSAT International X-ray Optical Survey (RIXOS). *MNRAS* 311, 456
39. Schwöpe A.D., Beuermann K., Catalán M.S., Metzner A., Steeghs D., R.C. Smith: 2000, Multi-epoch Doppler tomography and polarimetry of QQ Vulpeculae. *MNRAS* 313, 533
40. Tovmassian G., Greiner J., Schwöpe A.D., Szkody P., Schmidt G.D., Zickgraf F.-J., Serrano A., Krautter J., Thiering I., Zharykov S.: 2000, The new long-period AM Her system RX J2157.5+0855. *Astrophys. J.* 537, 927
41. Vrielmann S., Schwöpe A.D.: 2001, Accretion stream mapping of HU Aquarii. *MNRAS* 322, 269
42. Watson M.G., et al.: 2001, The XMM-Newton Serendipitous Survey I. The role of the XMM-Newton Survey Science Centre. *Astron. Astrophys.* 365, L51
43. Schwarz R., Schwöpe A.D., Staude A.: 2001, Photometry of the low accretion rate polar HS 1023+3900. *Astron. Astrophys.* 374, 189
44. Staude A., Schwöpe A.D., Schwarz R.: 2001, System parameters of the long-period polar V 1309 Ori. *Astron. Astrophys.* 374, 588
45. Schwöpe A.D., Schwarz R., Sirk M., Howell S.B.: 2001, The soft X-ray eclipses of HU Aqr. *Astron. Astrophys.* 375, 419
46. Schindler S., Castillo-Morales A., De Filippis E., Schwöpe A., Wambsganss J.: 2001, Discovery of depressions in the X-ray emission of the distant galaxy cluster RBS797 in a CHANDRA observation. *Astron. Astrophys.* 376, L27 (2001)
47. Schwöpe, A.D: 2001, Tomography of Polars. *Lecture Notes in Physics* 573, 127
48. Hambaryan V., Hasinger G., Schwöpe A., Schulz N.: 2002, Discovery of 5.16 s pulsations from the isolated neutron star RBS1223. *Astron. Astrophys.* 381, 98
49. X. Barcons, F.J. Carrera, M. Watson, ... A.D. Schwöpe, ...: 2002, The XMM-Newton Serendipitous Survey. II. First results on the AXIS high galactic latitude medium sensitivity survey. *Astron. Astrophys.* 382, 522 (2002)

50. Howell S.B., Ciardi D.R., Sirk M.M., Schwobe A.D.: 2002, Simultaneous EUV and IR observations of the eclipsing polar HU Aqr. *AJ* 123, 420
51. Schwobe A.D., Hambaryan V., Schwarz R.: 2002, A multiwavelength timing analysis of the eclipsing polar DP Leo. *Astron. Astrophys.* 392, 541
52. Schwobe, A.D., Brunner, H, Buckley, D.A.H., Greiner, J., v.d. Heyden, K., Neizvestny, S., Potter, S., Schwarz, R.: 2002, The census of cataclysmic variables in the ROSAT Bright Survey. *Astron. Astrophys.* 396, 895
53. Schwarz, R., J. Greiner, G. H. Tovmassian, S. V. Zharikov, and W. Wenzel: 2002. A new two-pole accretion polar: RX J1846.9+5538. *A&A* 392, 505-514.
54. A.D. Schwobe, H.-C. Thomas, R. Häfner, K.-H. Mantel, A. Staude: 2003, Cyclotron spectroscopy of HU Aquarii. *Astron. Astrophys.*, in press

6.2 Nichtreferierte Publikationen

1. Buckley D.A.H., Stobie R.S., O'Donoghue D., Schwobe A.D., Vennes S., Wickramasinghe D.T.: 1997, On the unusual nature of two EUVE magnetic CVs. *ASP. Conf. Ser.* 137, S.B. Howell, E. Kuulkers & C. Woodward (eds.), pp. 448-449
2. Hambaryan, V. V. 1998. On the Membership of Flare Stars in the Pleiades Cluster. *ASP Conf. Ser.* 154, 1492.
3. Hambaryan, V., R. Neuhäuser, and B. Stelzer 1999. X-ray Flares on the UV Cet Type Stars. *ASP Conf. Ser.* 188: Optical and Infrared Spectroscopy of Circumstellar Matter 155.
4. Stelzer, B., R. Neuhäuser, and V. Hambaryan 1999. X-ray Flares in Taurus-Auriga-Perseus. *ASP Conf. Ser.* 188, 151.
5. Schwarz, R. and J. Greiner 1999. Filling up the period gap: RX J0803.4-4748, a new 137 minute polar. *ASP Conf. Ser.* 157, 139.
6. Mirzoyan, L. V., V. V. Hambaryan, A. A. Akopian, A. V. Poghosyan, and G. N. Salukvadze 1999. On the expansion of stellar association Per OB2.. *Astrophysics* 42, 247-254.
7. Vriellmann S., Schwobe A.D.: 1999 Accretion Stream Mapping. Annapolis Workshop on Magnetic Cataclysmic Variables (MCV2), K. Mukai and C. Hellier (eds.), *ASP Conf. Ser.* 157, 93
8. Lehmann I., Hasinger G., Schwobe A.D., Boller Th.: 1999 AGN/galaxy separation in the ROSAT Bright Survey. in *Highlights in X-ray Astronomy*, MPE Report 272, pp. 209 – 212
9. Tovmassian G., Greiner J., Szkody P., Schmidt G.D., Schwobe A.D., Zickgraf F.-J., Krautter J., Thiering I., Serrano A., Zharykov S.: 1999 The new long-period AM Her system RX J2158+0855. *Proc. Brian Warner's 60th Birthday Colloquium*, in press
10. Hakobyan, A. A.; Hambaryan, V. V.; Poghosyan, A. V.; Salukvadze, G. N.: 2000 Two Expanding Groups of OB Stars in Stellar Association Per OB2. Birth and Evolution of Binary Stars, Poster Proceedings of IAU Symposium No. 200 on The Formation of Binary Stars, held 10-15 April, 2000, in Potsdam, Germany. Edited by Bo Reipurth and Hans Zinnecker, 2000, p. 124.
11. Greiner, J., D. H. Hartmann, W. Voges, T. Boller, R. Schwarz, and S. V. Zharykov 2000. Search for X-Ray Afterglows from Gamma-Ray Bursts in the RASS. *AIP Conf. Proc.* 526: Gamma-ray Bursts, 5th Huntsville Symposium 380.
12. Friedrich, S., Schwarz, R., Schwobe, A., Staude, A., Geckeler, R., Staubert, R.: 2000 Doppler-mapping of the Asynchronous Polars BY Cam and V1432 Aql. *AG Abstract Series* 17, P66
13. Hakobyan, A. A., V. V. Hambaryan, A. V. Poghosyan, and G. N. Salukvadze 2000. Two Expanding Groups of OB Stars in Stellar Association Per OB2. *IAU Symposium* 200, 124P.

14. DeFilippis, E., Castillo-Morales, A., Schindler, S., Schwöpe, A.D., Wambsganss, J.: 2001 Discovery of holes in the core of the distant galaxy cluster RBS797. XXXVth Rencontres de Moriond ‘Galaxy clusters and the high redshift universe observed in X-rays.’
15. König, B., R. Neuhäuser, and V. Hambaryan 2001. A Search for Young Nearby Stars. Astronomische Gesellschaft Meeting Abstracts 18, 703.
16. König, B., R. Neuhäuser, and V. Hambaryan 2001. A Search for Nearby Young Stars Among the Flare Stars. ASP Conf. Ser. 244, 87
17. Stelzer, B.; Neuhäuser, R.; Hambaryan, V.: 2001 X-ray Flares on Young Late-Type Stars in Taurus-Auriga-Perseus. ASP Conf Ser 223, 1171
18. Hambaryan, V., Schwöpe, A., Hasinger, G., Neuhäuser, R., Voges, W.: 2001 Variable Sources in the RASS: Bayesian Change Point Detection Approach. Mining the Sky, Proceedings of the MPA/ESO/MPE Workshop held at Garching, Germany, 31 July-4 August, 2000. Edited by A. J. Banday, S. Zaroubi, and M. Bartelmann. Heidelberg: Springer-Verlag, 2001., p.508
19. Hambaryan, V.; Hasinger, G.; Schwöpe, A. D.; Schulz, N. 2002 Discovery of 5.16 S pulsations from the isolated neutron star RBS1223. Mem. Soc. Astron. Ital., 73, 502-507
20. Gänsicke, B. T., H.-J. Hagen, J. Kube, R. Schwarz, A. Staude, D. Engels, D. Nogami, and M. Kuduz 2002. HS 0455+8315: A new eclipsing novalike variable. ASP Conf. Ser. 261, 623.
21. Schwarz R., Hedelt P., Rau A., Schwöpe A.: 2002 Tomography of AM Herculis. ASP Conf Ser. 261, 167
22. Staude, A., Schwarz R., Schwöpe A., Rau A.: 2002 Photometry with the Potsdam 70cm-telescope. ASP Conf Ser 261, 680
23. Schwarz R., et al: 2003 The new asynchronous polars RXJ0542+42. ASP Conf Ser, in press
24. Staude A., Schwöpe A., Schwarz R., Rau A.: 2003 Tomography of AM Herculis. ASP Conf Ser., in press

6.3 Eingeladene Review-Vorträge mit Angaben zu Publikationen

1. Eingeladener Reviewvortrag, 13th North American Workshop on CVs, Jackson Hole, Wyoming, USA, Juni 14 – 19, 1997
Schwöpe A.D., Beuermann K., Buckley D.A.H., Ciardi D., Cropper M., Horne K., Howell S., Mantel K.-H., Metzner A., Schwarz R., Sirk M., Steeghs D., Still M., Thomas H.-C.: 1997, Polars – multisite emission – multiwavelength observation. ASP Conf Ser 137, pp. 45–59
2. Eingeladener Reviewvortrag, Annapolis Workshop on Magnetic Cataclysmic Variables, Annapolis Maryland, USA, Juli 13 – 17, 1998
Schwöpe A.D., Schwarz R., Staude A., Heerlein C., Horne K., Steeghs D.: 1999, Tomography of polars. ASP Conf Ser 157, pp. 71–80
3. Eingeladenes Übersichtsreferat, DFG Rundgespräch *The future of cataclysmic variable research*, St. Andreasberg, Deutschland, Februar 21 – 24, 1999 (keine schriftliche Arbeit)
4. Eingeladener Reviewvortrag, *Astro-Tomography*, Brüssel, Belgien, Juli 5 – 7, 2000
Schwöpe A.D.: 2000, Tomography of polars. Lecture Notes in Physics 573, 127
5. Invited Review, *The Physics of Cataclysmic Variable and Related Objects*, Göttingen, Germany, August 5–10, 2001
Schwöpe A.D. et al.: LARPs – Low-Accretion Rate Polars. ASP Conf. Ser. 261, 102
6. Invited Review, *IAU Coll. 190 on Magnetic Cataclysmic Variables*, Cape Town, South Africa, Dec 8–13, 2002
Schwöpe A.D. et al.: Multiwavelength observations of eclipsing polars. ASP Conf. Ser. , in press

Appendix: Indirect Imaging of polars

7 Introduction

The physics of magnetic cataclysmic binaries (MCVs) differs fundamentally from nonmagnetic CVs due to the presence of a strong magnetic field. The field might prevent the formation of an accretion disk and dominate the internal dynamics of the binary. At sufficient low accretion rate and high magnetic field the spin of the accreting white dwarf becomes synchronized with the binary's period. MCVs come in two flavours, the *polars* with almost strictly synchronized accretors (degree of asynchronism less than $\sim 1\%$), and the *intermediate polars (IPs)* with observed spin periods of 68% to 0.1% of the binary period.

While the polars do not show any sign of an accretion disk, the IPs might possess a truncated disk. In both cases accretion onto the white dwarf occurs along magnetic field lines, either from the inner edge of the disrupted accretion disk or directly from the ballistic accretion stream. Magnetic accretion gives rise to intense X-ray radiation in the soft and hard X-ray regime from the footpoints of accreting field lines near the magnetic poles. X-rays are always pulsed with the spin frequency of the white dwarf due to self-occultation or fore-shortening of the X-ray emission region. In the polars, intense cyclotron radiation with sometimes resolved cyclotron harmonics dominates the optical spectra and yields additional information about the physical conditions in the accretion region. Most field strengths known today were derived by the identification of cyclotron harmonics.

Occasionally mass accretion ceases or is reduced substantially. During these episodes the optical spectra are dominated by the photospheres of the two stars. Particularly intriguing and challenging is the study of the photospheric Zeeman spectrum of the accretor. At the typical field strength encountered in polars, $B = 10 - 100$ MG, Balmer Zeeman lines are split by several hundred Ångströms, i.e. easily recognizable even in low-resolution spectra.

X-rays originating from the small accretion regions give rise to re-emission of high-excitation line radiation in the optical and the UV spectral range. The lines originate at all places in the binary systems exposed to the ionizing radiation, i.e. from the hemispheres of the donor stars facing the white dwarf and the different parts of the accretion streams or accretion curtains. Hence, a detailed analysis of the emission lines can reveal the whole dynamics and kinematics of such a binary system.

The binary periods of MCVs are rather short, they range from 78 min to 480 min for polars and from 84 min to 2 days for IPs. Most (2/3) of the polars appear below the period gap between 2 and 3 hours, the periods of IPs cluster between 3 and 6 hours. Most polars are as faint as 17th or 18th magnitude, only 10 objects have magnitudes equal to or brighter than 15th mag. This explains why observations with sufficient high time and/or spectral resolution for the application of tomographic methods are published for only a handful of systems so far. Nevertheless, the insight gained so far from, e.g. the application of Doppler tomography, is breathtaking and the level of detailed structure already discovered and to be explored in the future utilizing 8m-class telescopes on a micro arcsec resolution spatial scale highly promising.

In this review I firstly describe the results of Doppler tomography using bright emission lines observed in polars, both synchronously and asynchronously rotating. Accretion Stream Mapping, ASM, an eclipse mapping technique applied to emission from the accretion stream, is described in Sect. 9. ASM complements Doppler tomography, the results so far are not completely agreeing, the prospects for application of the combined approach, Eclipse Doppler Tomography, are discussed in Sect. 10. In the following Section 11 I describe the success of Doppler tomography using absorption lines from the photosphere of the secondary star in order to resolve the stellar disk of the donor.

The remaining parts of the review are devoted to the accreting white dwarf. The efforts there are focussed on two different structures, the hot accretion spot (Sect. 12) and the structure of its magnetic field (Sect. 13). The hot spot is investigated with classical eclipse mapping methods using optical and/or X-ray light curves of eclipsing or selfeclipsing systems. Hot spot imaging using cyclotron radiation needs still to be developed, a first approach, the so-called Stokes imaging, is described somewhere else in this volume (contribution by S. Potter). The magnetic field of the white dwarf often displays drastic deviations from the simple configuration of a centered dipole. First attempts and suitable systems are presented, which will allow mapping of the field structure in an objective manner (Sect. 13).

8 Doppler tomography of polars

8.1 Technical remarks

Doppler tomography implicitly assumes that emission is completely optically thin and bound to the orbital plane of the binary. The latter condition requires that systemic velocities have been removed from the data. Both prerequisites are violated in polars due to the presence of optically thick radiating or absorbing surfaces and the

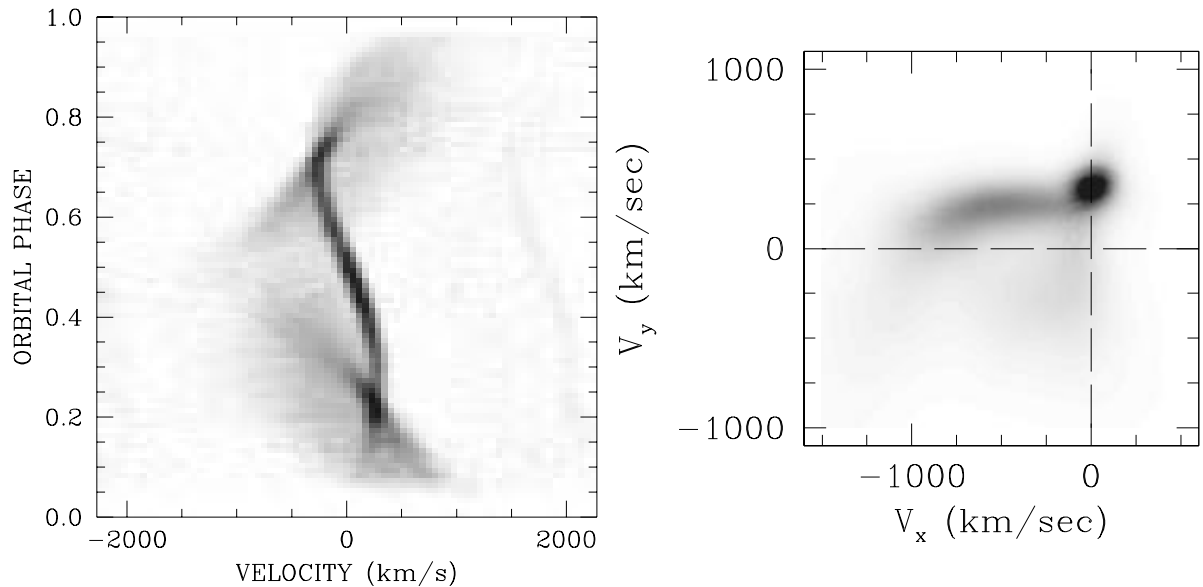


Abbildung 1: HU Aqr: Trailed spectrogram of He II $\lambda 4686$ and MEM-based reconstruction of the Doppler image in the 1993 high accretion state.

presence of out-of-plane velocities along magnetic field lines with $v_z \neq 0 \text{ km s}^{-1}$. Both these effects and limitations were discussed in more detail in Schwobe et al. (1999) and will not be reproduced here.

Published Doppler maps of polars are computed with either a Fourier-filtered back-projection algorithm (FFB) or a maximum-entropy minimization technique (MEM). In our Potsdam group we made experiments with the FFB-package kindly provided by K. Horne. It was originally developed for the analysis of disk systems, but was adapted to the analysis of non-disk systems and received an interface for MIDAS-input. A code for the construction of Doppler maps based on genetic optimization was developed in Potsdam, too, but converged very slowly compared to MEM-based algorithms. Also, Spruit's (1998) MEM-code freely made available via his web-page, was adapted to our needs and extensively used by us. The IDL-based graphic was replaced by a `pgplot`-based graphic, his spectral normalization was removed and a `perl`-based interface now allows data in-/output using `fits`-files. Most of the Doppler maps shown in this review are calculated with the slightly changed code of Spruit.

8.2 Doppler maps of polars

The first Doppler maps of a polar, VV Pup, and a suspected polar, GQ Mus, were published in 1994 by Diaz & Steiner (1994a, 1994b). These maps were based on intermediate resolution spectroscopy of H α and He II $\lambda 4686$ with a phase resolution slightly better than 0.1, i.e. with angular resolution of about 30° . Although not very high in resolution, they were showing the dramatic differences between Doppler maps of disk and diskless accretors and the great potential for future discoveries. They also allowed a rough separation of emission line flux originating on the irradiated secondary star and from the accretion stream. The first well-resolved Doppler map of a polar, HU Aqr, a high-inclination eclipsing system, was presented by Schwobe et al. (1997). The trailed spectrogram of He II $\lambda 4686$ used for the tomography experiment and the corresponding Doppler map are reproduced in Fig. 1.

The brightest emission lines of polars in their high accretion states are the Balmer lines and He II $\lambda 4686$, with the latter much less affected by optical depths effects than the Balmer lines. This makes the Balmer lines intrinsically broader and the corresponding Doppler maps show less structure. For this reason I am referring in this article mostly to He II $\lambda 4686$ maps.

The Doppler map shown in Fig. 1 clearly shows three different structures which are not so easily recognizable in the trailed spectrogram. Easily interpretable is the emission spot at $(v_x, v_y) = (0, 300) \text{ km s}^{-1}$, which is the Doppler image of the pronounced s-wave emission of the dominant narrow emission line. A cometary tail linked to it stretching down to $v_x \simeq -1000 \text{ km s}^{-1}$ and a diffuse patch of emission in the lower left quadrant are the two further structures mentioned. Parallel projections of elongated structures like the cometary tail yield very broad lines, FWHM up to $\sim 1000 \text{ km s}^{-1}$, at certain phases (0.0 and 0.5 in the present case), whereas at phases 0.25 and 0.75 such projections result in rather narrow features of full width at half maximum (FWHM) of only about 200 km s^{-1} . This means that one easily might lose track of certain features in trailed spectrograms and arrive at misleading conclusions if sinusoids are fitted to radial velocity curves of Gaussian-fitted emission lines.

A basic understanding of the Doppler maps of polars in general and of HU Aqr in particular can be reached

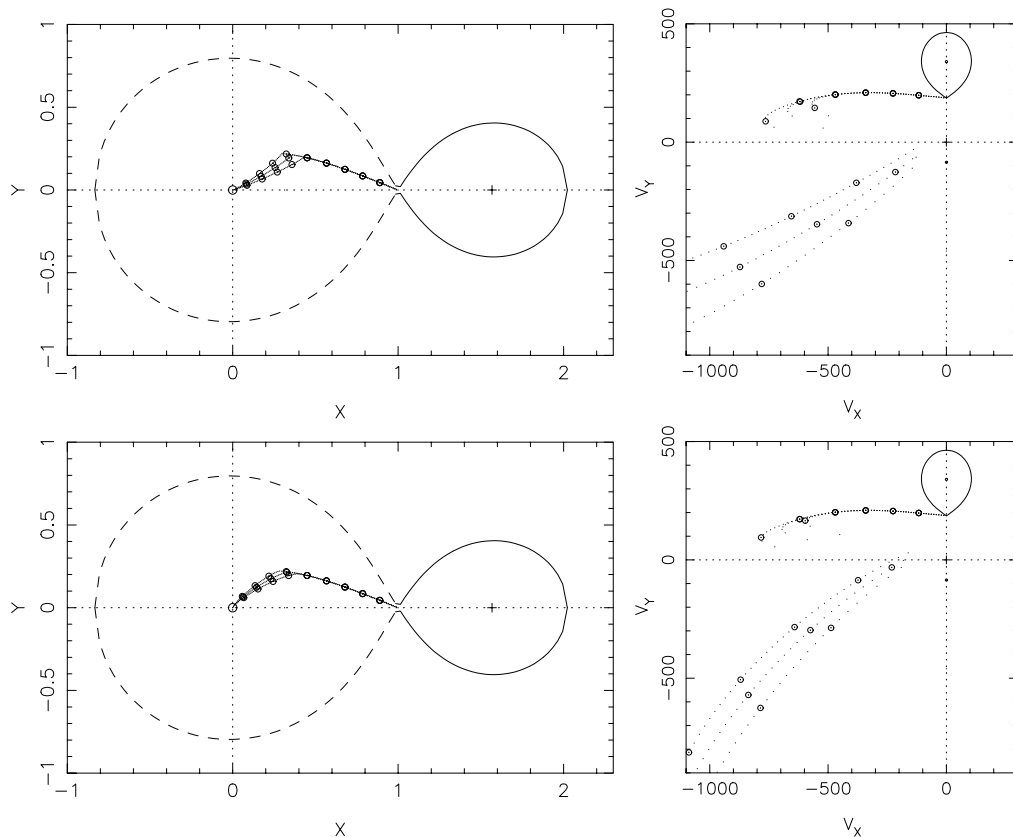


Abbildung 2: Schematical representation of a simple accretion geometry in true spatial (left) and Doppler coordinates (right). The inclination of the dipole axis with respect to the rotation axis is 15° , in the upper row it is tilted towards the secondary star, in the lower row perpendicular to the line joining both stars.

by plotting the orthogonal components of the velocity vectors typically encountered in a polar system in a two-dimensional plane. One usually plots the projections of orbital and streaming velocities onto the orbital plane (Fig. 2). As usual, the x -axis of the coordinate system runs through the centres of both stars, the y -axis lies in the orbital plane and the z -axis parallel to the rotational axis.

Emission line radiation, particularly from species with a high ionization potential like He II $\lambda 4686$, is mainly of reprocessed photoionized origin. This kind of radiation is expected to be emitted from those places in the binary system, which are irradiated by X-rays from the accretion spot. Three distinctly different structures may be expected in a Doppler map of polar, if one accepts the basic picture of the accretion geometry as shown in Fig. 2. Firstly, there is the heated front side of the secondary star, secondly the ballistic part of the accretion stream and finally the magnetically dominated part of the accretion stream. The comparison with Fig. 1 reveals that these structures indeed can be observed in nature. The computations which led to Fig. 2 assume that emission from the secondary star originates from the Roche surface. The ballistic stream was defined by a single-particle trajectory. These assumptions can be tested by observations. The computations which led to the figure further assumed that the stream follows a particle trajectory until the magnetic pressure of the magnetic field overcomes the ram pressure in the stream. In that threading region the velocity component along the magnetic field is conserved, the other components are neglected. Depending on the assumed orientation of the dipole this then leads to significant jumps of the trajectory in Doppler space. The jumps become large, if the magnetic axis is roughly aligned with the rotation axis. The trajectory 'turns smoothly around the corner', if the dipole axis is highly inclined. In Fig. 2 I compare two situations with the same inclination of the dipole axis with respect to the rotation axis but with an azimuth differing by 90° . The velocity jump from the end of the ballistic stream at $(v_x, v_y) \simeq (-800, 100) \text{ km s}^{-1}$ to a velocity near the origin is almost the same in both cases, differences become obvious at higher velocities in the magnetic stream (lower left quadrant of the diagram). Under lucky circumstances the magnetic stream can be made visible in Doppler maps and the orientation of the field which guides matter down to the white dwarf can be determined. Further below I will discuss two such examples (UZ For, AR UMa).

The location of the secondary star and of the ballistic stream in the Doppler map are dependent on the mass

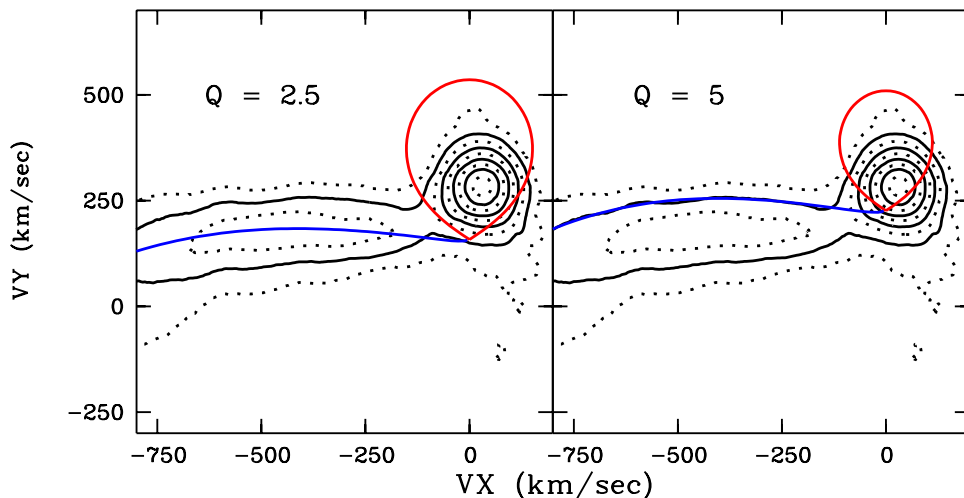


Abbildung 3: Contour plot of the HeII $\lambda 4686$ Doppler map of HU Aqr with Roche lobes and ballistic streams overlaid according to given mass ratio Q .

ratio and the absolute masses of the stars in the binary. Doppler tomography thus may potentially be used to determine masses of the binary by locating the ballistic stream in a Doppler map. These expectations could not be fulfilled so far. The interpretation of the Doppler maps turned out to be more complicated than suggested by the simple geometrical picture. This became evident already in HU Aqr, where the optimal mass ratio which reflects the location of the ballistic stream was only $Q = 2.5$ and the optimal mass ratio for the irradiated side of the mass-losing star $Q = 5$ (Fig. 3).

Taking into account the detailed shape, i.e. length of the optical and X-ray eclipse and the radial velocity amplitude of the secondary star measured using the near infrared NaI $\lambda 8183/8194$ lines (see Sect. 11), the mass ratio turned out to be $Q \simeq 4$. This means that in the case of HU Aqr neither the ballistic stream, which is, compared to other polars, an extraordinary distinct structure in the Doppler map, nor the narrow emission line from the secondary star fit straightforwardly in the simple picture outlined in Fig. 2.

The long-period polar QQ Vul shows an even more drastic and variable disagreement between the simple picture and the observed location of the ballistic accretion stream. In Fig. 4, adapted from Schwöpe et al. (2000), the HeII $\lambda 4686$ Doppler maps obtained at three different epochs are compared.

In 1986 no ballistic stream can be recognized, which in part can be explained by the fact that this particular data set has the lowest spectral and time resolution of the three sets shown. However, the maps of 1991 and 1993 clearly show structures which look like emission from the ballistic stream. But this kind of emission was observed at variable velocity v_y ($v_y = 45 \text{ km s}^{-1}$ in 1991, $v_y = 0 \text{ km s}^{-1}$ in 1993) which cannot happen, if it would originate from a single-particle trajectory starting at the inner Lagrangian point L_1 .

There are two possibilities to cure the problem of dislocated 'ballistic' streams which are in all observed cases shifted towards lower than the nominal v_y -velocity for a given Q . Both possibilities involve magnetic fields as the likely cause, either that of the secondary or that of the primary star. The field of the secondary near L_1 is of the order of the field strength of the primary at that location. Hence it could have a large effect on the stream trajectory near the L_1 point. Matter near the L_1 point can either be deflected by the combined magnetic field of both stars or trapped in a slingshot prominence and released at a location and velocity very different than that of the L_1 . Using HST-based Doppler tomography of bright UV lines in AM Herculis itself, Gänsicke et al. (1998) showed the presence of highly ionized gas with low velocity dispersion corotating with the binary and located between L_1 and the centre of mass. This was explained as evidence for the occurrence of a magnetic slingshot prominence emanating from the secondary star, similarly to the dwarf novae IP Peg and SS Cyg (Steehs et al. 1996).

A different approach was followed by Sohl & Wynn (1999) who modelled the accretion flow as an ensemble of diamagnetic blobs interacting independently with the magnetosphere of the primary. Their interaction term takes the form of a velocity-dependent surface drag force per unit mass, $f_{\text{drag}} = -k\vec{v}_r$, with \vec{v}_r the relative velocity of the blob across the field line and $k \propto \mu^2(\rho_b l_b)^{-1}$ the drag coefficient ($\vec{\mu}$: magnetic moment of the white dwarf, ρ_b : blob density, l_b : blob length scale). This approach allows the magnetic stresses to vary continuously as each blob accelerates towards the secondary and thus raising an accretion curtain in 3D. This step of modelling needs to be elaborated, the first trailed spectra presented by Sohl & Wynn were calculated for fixed k for all blobs and, when

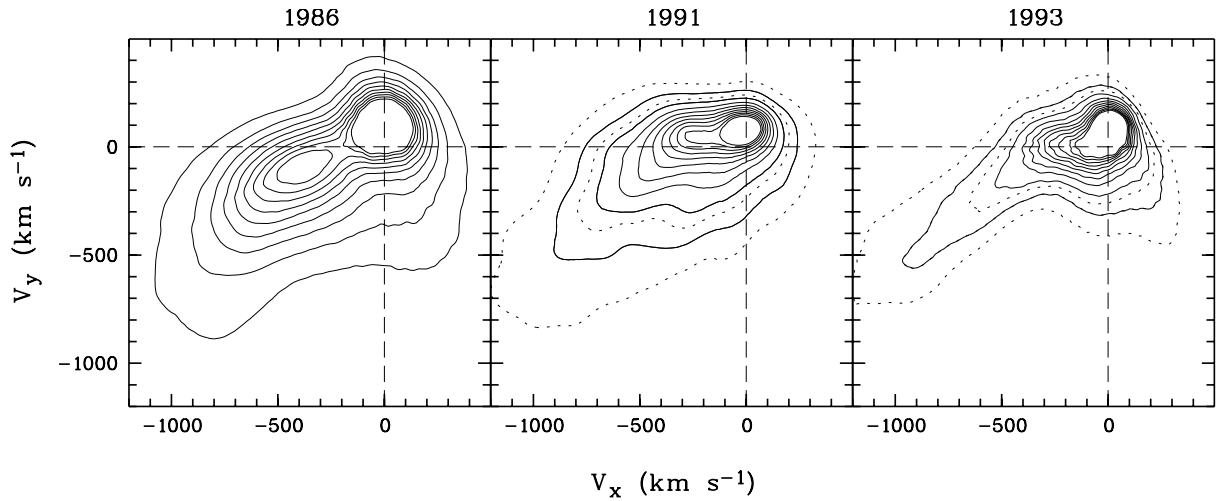


Abbildung 4: QQ Vul: Comparison of Doppler maps in the line HeII $\lambda 4686$ obtained at epochs as indicated in the Figure.

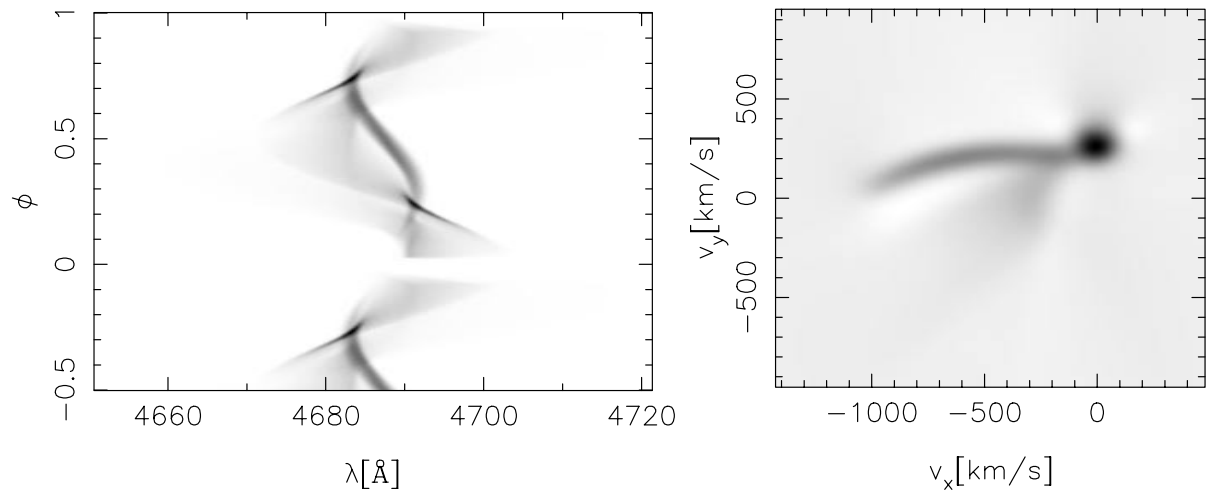


Abbildung 5: Trailed spectrogram and Doppler map of HU Aqr according to Heerlein et al. (1999); to be compared with the observed trailed spectrum and Doppler map shown in Fig. 1.

applied to HU Aqr, left systematic residuals in the trailed spectrograms. Only after improvement by allowing e.g. k to be variable, the question can be answered if the model yields clues to the problem of dislocated ballistic streams.

Another accretion curtain model was developed by Heerlein et al. (1999) for HU Aqr who raised it by assuming a two-dimensional Gaussian density distribution in the ballistic stream, which becomes stripped if the magnetic pressure at a given place exceeds the sum of ram and thermal pressures. Assuming a constant surface density in the curtain, the ballistic stream and on the secondaries surface, they optimized their solution with a χ^2 -fit and solved mainly for geometrical parameters. Their modelled trailed spectrogram and Doppler map is shown in Fig. 5, when subtracted from observed data (Fig. 1) both, the trailed spectrogram and the Doppler map, show systematic residuals, which are particularly pronounced at the ballistic stream and the unshielded secondary star. This means that their dynamical model as well as the assumption of constant surface brightness along the ballistic and the magnetic stream are clearly much too simple.

The presence of an accretion curtain in HU Aqr, which makes proper modelling of the trailed spectrograms so difficult, is revealed indirectly also by the asymmetry of line radiation originating from the secondary star, both in high and low accretion states (see Fig. 6, adapted from Schwope et al. 1999). In both Doppler maps the centroid of light lies on the trailing (right) side of the Roche lobe, which means that the leading side is less affected by irradiation, i.e. shielded by an accretion curtain. This view is supported by soft X-ray observations of HU Aqr,

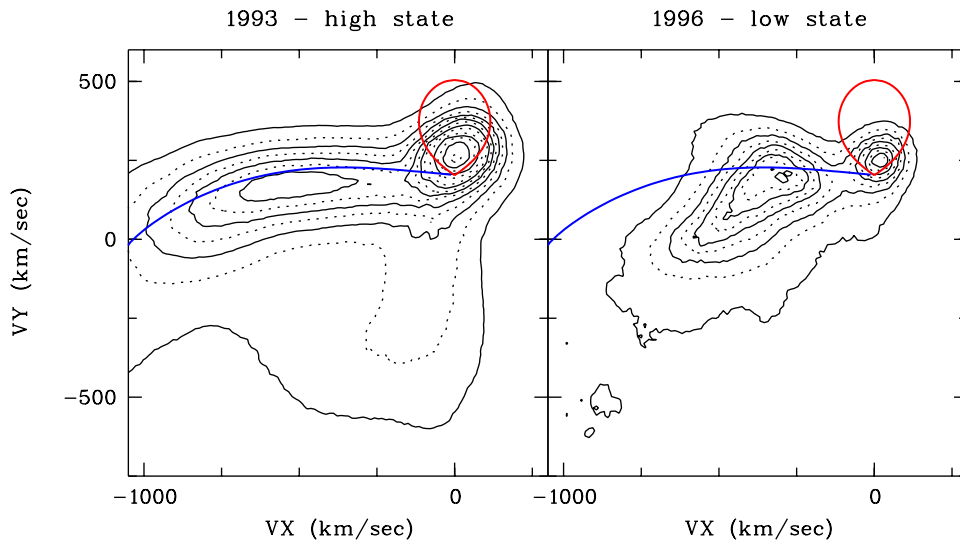


Abbildung 6: Comparison of the 1993 high and the 1996 low state Doppler map of the eclipsing polar HU Aqr (Schwope et al. 1999).

which show attenuation of the X-ray flux prior to the eclipse, when the curtain blocks the view down to the hot accretion spot.

Exploring Doppler maps of Polars: UZ For

UZ For is in many respects a twin system to HU Aqr, it has a period of 126.5 min, similar to the 125 min of HU Aqr, close to the lower edge of the period gap, it has a not too different magnetic field strength in the main accreting pole (53 MG compared to 36 MG) and, most important here, it is an eclipsing system with inclination of about 81° (compared to $\sim 85^\circ$ for HU Aqr). The main difference is, that UZ For is a proven two-pole accretor, the second pole having a significantly higher field strength of ~ 75 MG (Schwope et al. 1990). The existence of a second accreting pole derives from the presence of cyclotron lines from this second region and from detailed eclipse photometry (Bailey 1995), which shows a two-step ingress and egress at optical wavelength attributed to two accretion regions. Interestingly, at X-ray wavelengths (ROSAT and EUVE observing windows) only one accretion region is evident, thus demonstrating the large temperature difference in the two regions.

The Doppler map of UZ For shown in Fig. 7 clearly shows three different emission structures, the irradiated front side of the secondary star, emission which is associated with the ballistic accretion stream and emission from the magnetically controlled part of the stream in the lower left quadrant. We modelled the stream emission with the same model which led to Fig. 2. With a co-latitude of the magnetic axis $\delta = 15^\circ \equiv 165^\circ$ and an azimuth $\varphi = 45^\circ$ excellent agreement between the observed and modelled location of the stream can be reached. The three trajectories shown in Fig. 7 couple onto magnetic field lines $\varphi = 10^\circ - 20^\circ$ prior to eclipse centre. These parameters predict a location of the accretion spot at co-latitude $26^\circ (\equiv 154^\circ)$, azimuth 31° , and the occurrence of an X-ray absorption dip at phase 0.96. The spot co-latitude predicted is in good agreement, the azimuth and dip phase disagree with the detailed EUVE-observations by Warren, Sirk & Vallergera (1995). They observed the dip at phase 0.91 and the spot at an azimuth of 49° . This leaves us with three possibilities: (1) our modelling is insufficient, or (2) the stream that we are seeing in the Doppler maps feeds the secondary accretion spot which is not seen by EUVE and ROSAT, or (3) the disagreement is due to a pronounced re-arrangement of the accretion geometry. Without simultaneous observations in the X-ray and the optical wavelength range it will be difficult to discern between the different options. A further complication arises: For the computation of the model trajectories we assumed a mass ratio $Q = 3$, thus achieving a convincing fit. This mass ratio differs from the best-fit value, $Q = 5$, obtained by Bailey & Cropper (1991) from eclipse light curve modelling. At higher mass ratio the secondary's Roche lobe is shifted upwards in Doppler space. Then the spot of emission originating from the secondary star is located near the L_1 and not on the irradiated surface, and the observed ballistic stream is dislocated with respect to the ballistic trajectory towards smaller v_y , similarly as in HU Aqr and in QQ Vul. Proper understanding and modelling of the Doppler map if UZ For requires an accurate determination of the mass ratio.

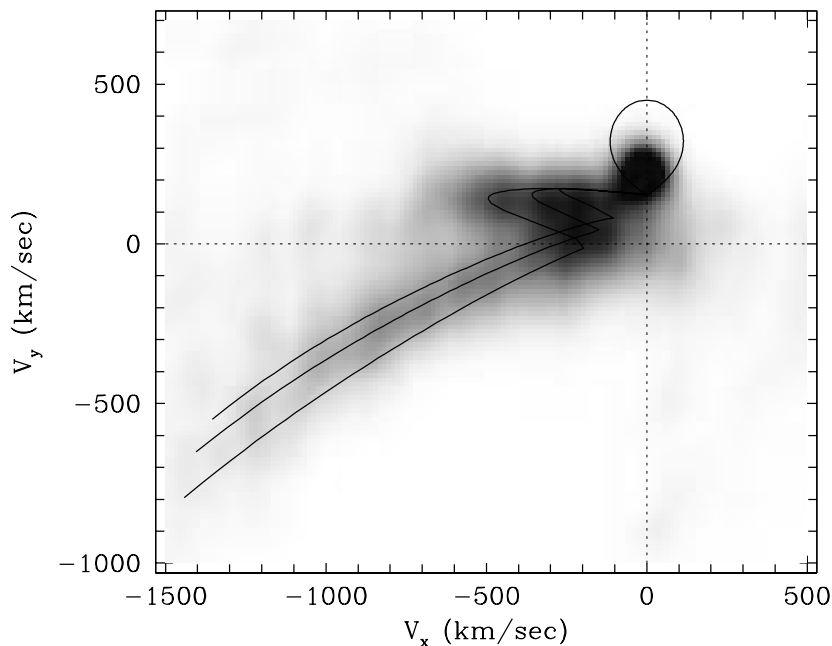


Abbildung 7: Doppler map of UZ For in the HeII $\lambda 4686$ emission line. Clearly visible are the irradiated front side of the secondary star, the ballistic stream and the or a magnetically coupled stream (Schwope et al. 1999).

Exploring Doppler maps of Polars: AR UMa

For more than a decade the measured field strength of polars were distributed between 10 MG and 70 MG and remained clearly below 100 MG. Then, in 1996, Schmidt et al. detected in a low-resolution IUE-spectrum of the $P_{\text{orb}} = 115$ min *Einstein* source 1ES1113+432 (now called AR UMa) flux depressions near $L\alpha$ which were interpreted as Zeeman split $L\alpha$ absorption lines in a field of 230 MG, thus breaking the 100 MG barrier for the first time. The interesting question arose, whether in such a high-field system accretion happens via the classical path with a ballistic and a magnetic accretion stream or whether matter leaving the secondary star would couple onto magnetic field lines directly at the L_1 -point. This question was answered by Doppler tomography (FFB, Schmidt et al. 1999), showing the typical feature of a ballistic stream connected to the irradiated hemisphere of the secondary star.

A MEM-based Doppler map of the data presented by Schmidt et al. of the HeII $\lambda 4686$ line is reproduced in Fig. 8. Besides the irradiated secondary which allowed proper phasing of the spectra the maps shows clearly some kind of ballistic stream and a magnetic stream.

Doppler tomography allows to derive the far-field accretion geometry, i.e. far away from the white dwarfs surface. The results achieved can be compared with results obtained from polarimetric observations which allow to derive the near-field accretion geometry. Such a comparison is made in Fig. 8. The parameters used for computation of the single-particle shown in the figure are: orbital inclination $i = 50^\circ$, co-latitude of the magnetic axis $\delta = 45^\circ$, azimuth of the magnetic axis $\chi = 80^\circ$, mass ratio $Q = M_1/M_2 = 3.8$ (fixed parameter). The mass of the white dwarf M_1 was fixed at $0.7 M_\odot$.

Schmidt et al. (1999) derived $i = 40^\circ - 60^\circ$, $\delta = 35^\circ - 10^\circ$, and $\chi = 90^\circ \pm 7^\circ$. For $i = 50^\circ$, used for our example in Fig. 8, they predict $\delta \simeq 20^\circ$ (depicted from their Fig. 5). Such a low value of δ is not compatible with our modelling of the Doppler map. For all possible values of i we had to assume higher values of δ (by $10^\circ - 20^\circ$) than compatible with the results from polarimetry. Doppler tomography and polarimetry consistently confirm a very high azimuth of the magnetic axis.

A cautious remark is in place. In the high state of the system there are likely two streams present feeding the two poles, and this might confuse the tomogram analysis for the magnetically-controlled parts of the stream.

Apart from these difficulties, Doppler tomography seems to help to further constrain the possible ranges of the mass ratio, the orbital inclination and the co-latitude of the magnetic axis.

Similarly to the systems discussed above, the structure which we refer to as 'ballistic stream' in the Doppler map is significantly broader (extended towards smaller v_y) than predicted by the single-particle model. Again, this seems to be indicative of an accretion curtain. Without further information other than provided by the Doppler

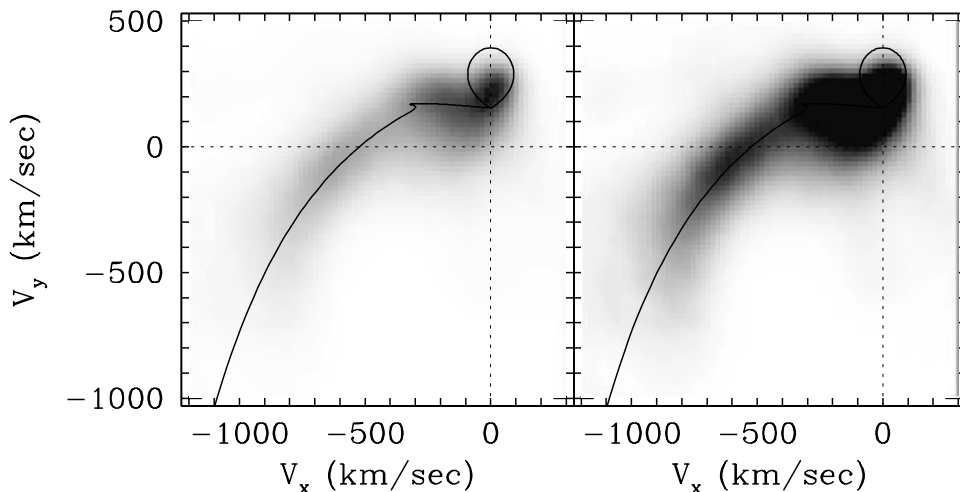


Abbildung 8: MEM-based Doppler map of AR UMa in the HeII $\lambda 4686$ emission line. The same map is shown twice using different intensity cuts. The spectral data were kindly made available by G. Schmidt.

tomogram (which is based primarily on gaseous optically thin radiation) we cannot judge whether the bulk of matter is transferred via the accretion curtain or via the magnetic stream, which is seen in the lower left quadrant of the map. But the clear existence of a structure like a magnetic stream supports the idea that even in a high-field system like AR UMa the mass transfer between the two stars happens in a rather conventional way.

Exploring Doppler maps of Polars: V1309 Ori

V1309 Ori (= 1RX J0515.41+0104.6) is the polar with by far the longest binary period, $P_{\text{orb}} = 7.98$ hours (Walter et al. 1995, Shafter et al. 1995). It contains a slightly evolved secondary of spectral type M0.5III. Fortunately, the system has a high binary inclination of about 78° (Staudte et al. 2000, in preparation) and is eclipsing. The eclipses, which might last as long as 46 mins, display large variations of their length thus immediately demonstrating that the source of emission which becomes obscured is not a structure of fixed size, like e.g. the white dwarf, but a transient structure like an accretion stream or accretion curtain in the magnetosphere of the white dwarf primary.

Doppler maps of V1309 Ori using the two Helium lines (4686\AA and 8236\AA) are displayed in Fig. 9. The HeII $\lambda 4686$ map shows the meanwhile well-known feature of an irradiated secondary and an elongated structure of emission from the accretion stream and/or curtain. Ballistic and magnetic stream do not emerge as separate structures. The ballistic stream is faint between $v_x = 0 \text{ km s}^{-1}$ and -200 km s^{-1} . The broad, extended structure centred on $(-300, 0) \text{ km s}^{-1}$ must be emission mainly from the magnetic dominated part of the accretion flow because of its low v_y velocity. The map of the near infrared line (HeII 8236\AA) is qualitatively different. Emission from the secondary is very weak and hardly separable from stream emission. The ballistic stream in HeII $\lambda 8236$ is bright where the stream in HeII $\lambda 4686$ is faint. A second isolated spot of emission appears at $(v_x, v_y) = (-420, 30) \text{ km s}^{-1}$, where the ballistic stream probably reaches its final end and dissipative heating becomes important for excitation. No detailed modelling of the maps is available so far but the maps constructed from different ionization stages and atomic species bear a great potential for modelling yet to be explored. However, such computations are rather difficult to be performed due to the high particle density in the stream, the unknown density structure and the anisotropic absorption cross sections of matter in the stream due to the high flow velocities.

Exploring Doppler maps of Polars: The asynchronous rotators BY Cam and V1432 Aql

Most MCVs of AM Her subtype rotate, by definition, synchronously. There is, however, a small subgroup of presently only four confirmed systems (out of 67 polars known to me) which rotate slight asynchronously. Their spin and orbital periods typically differ by only about one per cent (see Campbell & Schwope 1999 for more details). There might be more such systems, the discovery of an asynchronism makes long photometric monitoring necessary and also the independent determination of the true orbital period, preferably by spectroscopy. Long-term photometry is lacking for most of the recently (ROSAT-)discovered and even for most systems known from the pre-ROSAT era.

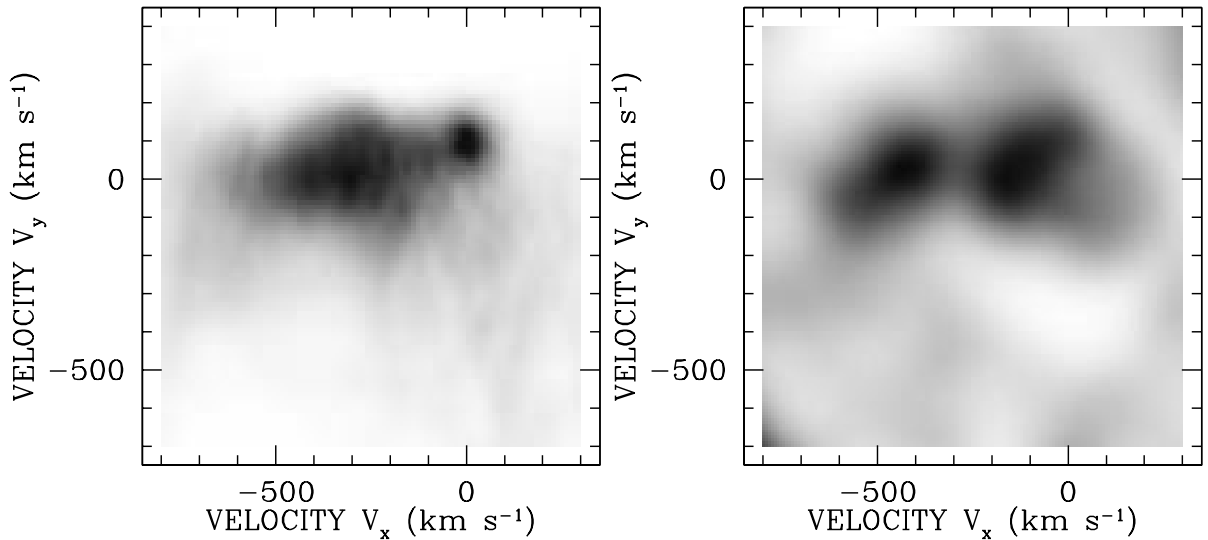


Abbildung 9: Doppler maps of V1309 Ori obtained in November 1995 in the lines of He II $\lambda 4686$ (left) and He II $\lambda 8236$ (right).

It is not known how mass exchange works in asynchronously rotating polars, e.g. if always only one, or always both poles are accreting or if a pole-switching scenario applies. This question can be tackled by Doppler tomography and the results can be compared with spin-phase resolved tomography of the emission lines in IPs presented by Hellier (1999). These show either one or two accretion curtains, some of them with opening angles of more than 100° .

Twice, in November 1998 and December 1999, we tried to follow the evolution of Doppler tomograms of BY Cam through a beat cycle between spin and orbital period, unfortunately at both occasions bad weather conditions allowed only a snapshot at one beat-phase to be taken (Schwarz et al. 2000, in preparation). The $H\beta$ map of BY Cam obtained in November 1998 is shown in Fig. 10. The map is compared with a Doppler map of V1432 Aql, the only known magnetic CV which has a spin period longer than the orbital period. The spectral data of V 1432 Aql used for computation of the map were kindly provided by S. Friedrich, R. Staubert, and R. Geckeler.

The spectra of BY Cam allowed for the first time proper phasing of the data by tracing the secondary star via quasi-chromospheric emission from its irradiated front side. The map displays no clear signature of a ballistic or a magnetic stream. Instead, emission is widely spread in the (v_x, v_y) plane with some degree of symmetry around the v_y -axis. Particularly striking is the simultaneous detection of red- and blue-shifted emission at phases 0.0 and 0.5, which is reminiscent of an accretion disk. The Doppler image of a disk, however, is a ring or torus centred on the velocity of the white dwarf, clearly different from the map of BY Cam (for a collection of Doppler maps of accretion disks see e.g. Kaitchuck et al. 1994). Although no clear and detailed picture for the emission of BY Cam could be developed so far, the Doppler map suggests that some kind of extended accretion curtain is present with opening angle between 180° and 360° .

The map of V1432 Aql, which has lower resolution and lower signal-to-noise, but shows a similar structure with red- and blue-shifted emission being simultaneously present at phases 0.0 and 0.5. Our understanding of these structures is still in its infancy. The similarity of the two maps suggest, that a common lesson can be learnt from a thorough study of asynchronously rotating polars.

9 Accretion stream mapping (ASM)

A second approach to model the brightness distribution along the accretion stream was developed recently by three independent groups. They make use of photometric data only (instead of spectrally resolved data). Classical eclipse mapping methods, which were originally applied to flat accretion disks, were modified by these groups and applied to a stream in threedimensional space. All methods invert a given light curve and map it onto an accretion stream with pre-defined geometry. This is in all recent cases a ballistic stream described by a single-particle trajectory and a dipolar field line connected to it. The methods differ mainly with respect to the kind of data which are used. Two systems, the twins HU Aqr and UZ For, were studied so far.

Hakala (1995) and Harrop-Allin et al. (1998, 1999) used broadband $UBVR$ -photometry of HU Aqr in low and high accretion states (examples of such light curves are shown in Fig. 11). They made use of data around eclipse

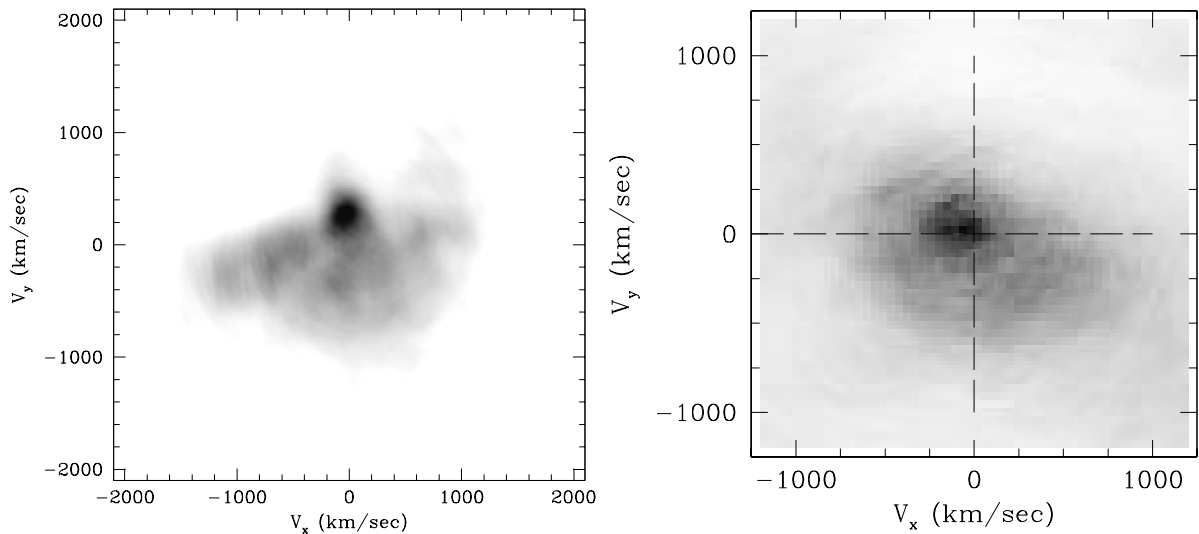


Abbildung 10: Doppler maps of the asynchronous rotators BY Cam (left, Balmer $H\beta$) and V1432 Aql (1RX J1940-10, right, HeII $\lambda 4686$) at one certain beat phase.

phase thus regarding in their inversion process the eclipse by the secondary star only as determining the visibility function.

Similarly, Kube et al. (2000) used HST/FOS observations of UZ For around eclipse phase and mapped the light curve of the CIV $\lambda 1550$ emission line. By using emission line data instead of broadband continuum data one avoids contaminations by the stellar photospheres, by cyclotron radiation from the hot accretion spot and by photospheric continuum radiation from the accretion spot. Cyclotron radiation and spot emission have angular-, thus phase-dependent brightness, which leads to asymmetric eclipse light curves. This clearly complicates the mapping process and emission line data therefore should be used whenever available. On the other hand, broadband data are typically available with better signal-to-noise and higher time resolution than spectrally resolved data.

Vrielmann & Schwope (2000) finally mapped Balmer ($H\beta$, $H\gamma$) and HeII $\lambda 4686$ emission line light curves of HU Aqr in its high accretion state and made use of the full orbital light curve. Contrary to the other teams, they treat the accretion stream as a true three-dimensional structure (a twelve-sided tube), thus allowing for different brightness on the irradiated and non-irradiated sides of the stream. This was found to be necessary because the observed emission line light curves displayed pronounced optical depth effects (see Fig. 11).

Results of the latter work are reproduced in Fig. 12. The brightness map shows a bright spot at the stagnation region, where the stream becomes redirected and couples onto magnetic field lines suggesting pronounced dissipative heating in the coupling region. A projection of the best-fit map with high phase resolution, however, shows that this feature seems to have exaggerated brightness in the map. It is responsible for the hump in the predicted light curve just before the eclipse of the stream becomes complete (phase -0.027). Since the mapping algorithm stably found the same solution, irrespective whether noise was artificially added or only data from a restricted phase interval were used for the mapping experiment, this is suggestive of a more complex accretion geometry than used for the experiment. The existence of an accretion curtain in HU Aqr was mentioned above already. A numerical experiment performed by Vrielmann & Schwope in order to map the observed light curve onto an accretion curtain failed however, because the number of degrees of freedom in a curtain was found too large in order to constrain the fit. A complete picture of the stream thus makes higher time resolution emission line data with spectral resolution necessary.

Although investigating the same object, HU Aqr, at the same epoch, new moon in August 1993 (the observations were performed during the same nights from observatories in Spain and Texas), the maps by Vrielmann & Schwope differ clearly from those by Harrop-Allin et al., the latter showing a pronounced brightness increase towards the white dwarf. I ascribe this difference mainly to the use of the different kind of data: broadband photometry including contaminating radiation from the white dwarf by Harrop-Allin et al. vs. emission line flux from the stream only by Vrielmann & Schwope.

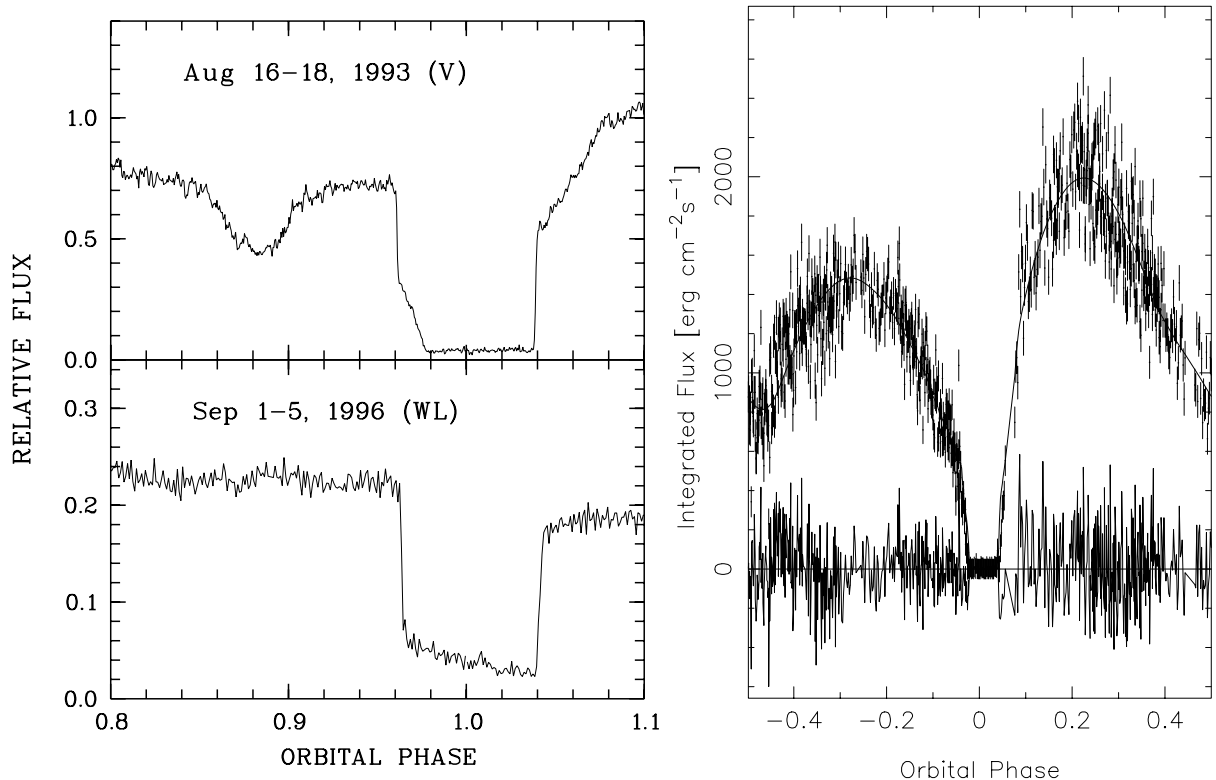


Abbildung 11: (left) Optical light curves of HU Aqr in high (top) and low (bottom) accretion states. The high state light curve was obtained in the optical V-band with the high-speed multicolour photometer MCCP at the Calar Alto 2.2m telescope in August 1993 (time resolution 0.5 sec), the low state light curve taken in white, i.e. unfiltered light, was obtained with the 70cm telescope at the AIP in Potsdam-Babelsberg in September 1996 (time resolution 15 sec).

(right) Integrated light curve of He II $\lambda 4686$ of HU Aqr in its high accretion state. The spectral data were taken simultaneously with the high-speed photometry in the top left panel (adapted from Schwöpe et al. 1997). The solid line through the data points is based on ASM by Vrielmann & Schwöpe (2000).

10 Eclipse Doppler Tomography

In the previous section the difficulties preventing us from successfully mapping an observed light curve on an accretion curtain were mentioned. The final reason for the failure is the lack of data with high time and spectral resolution all along the eclipse of the curtain and the stream. This situation will be changed in the era of 8-10m class telescopes. Instead of inverting the observed light curve of a spectral line in integral light, it will become possible to make use of the simultaneously recorded velocity information, i.e. to perform ASM in a velocity bin. A first attempt in this direction was undertaken recently by Bobinger et al. (1999) and Bobinger (2000) who investigated the accretion disk structure in IP Peg. They performed a *double dataset eclipse mapping*, using trailed spectra outside eclipse and broadband photometry at eclipse phase.

The approach proposed here foresees usage of one dataset only, namely the phase-dependent flux $F_{v,\varphi}$ at velocity v in a selected spectral line which can be expressed as

$$F_{v,\varphi} = f(d) \sum_{j=1}^M I_j(v) \xi_{j,\varphi} a_{j,\varphi} \quad (1)$$

with $f(d)$ being a scaling factor (i.e. distance-dependent), $I_j(v)$ the intensity at the pixel j with velocity v in the curtain, M the number of the pixels, $\xi_{j,\varphi}$ the visibility function, $a_{j,\varphi}$ the projected area of the pixel and φ the orbital phase. The geometry of the curtain has to be defined, the inversion of a trailed spectrogram then will yield a map $I_j(v)$.

One difficulty one will encounter is the unknown velocity field in the curtain (contrary to disk systems, where a Keplerian velocity field can be assumed). One may think of different options which can be tested. The first

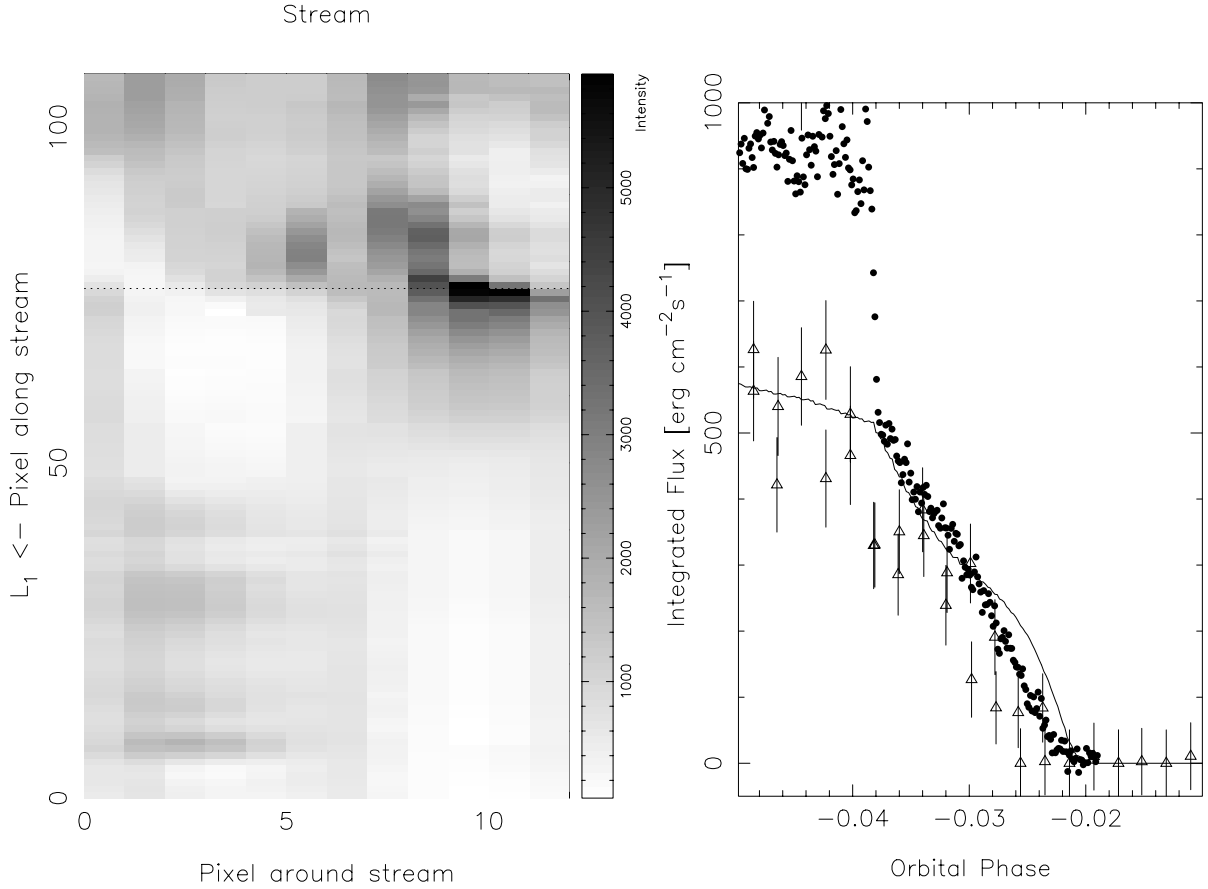


Abbildung 12: (left) ASM-based brightness map along and around the accretion stream of HU Aqr in its high accretion state (Vrielmann & Schwope 2000).

(right) Projected stream brightness map of HU Aqr in comparison with the input data (few data with large error bars) and with high time resolution broadband MCCP-data.

conserves the velocity component along the local magnetic field in the coupling region for a given stream element (as was done above in Fig. 2), the second dissipates the kinetic energy of a stream element completely and uses as initial velocity along a given field line the mean kinetic energy in the coupling region. Despite these difficulties *Eclipse Doppler Tomography* is the logical next step in order to overcome the shortages of mapping experiments making use of light curves in integral light. One preferentially uses for such an experiment a long-period polar with reasonably long ingress and egress phases, like e.g. V1309 Ori or EUVE J1429-38.

11 Doppler maps of donor stars in MCVs

Polars show in their spectra features of the donor star if the contribution of that star to the summed light makes a significant contribution, i.e. if it is not outshone by accretion-induced radiation. This happens in long-period systems with their big secondaries even in high states and it may happen in short-period systems if the accretion rate is reduced, i.e. if they have entered a low accretion state. If spectral signatures of the secondary can be traced through the orbital cycle, the radial velocity information can be used for an accurate determination of the binary period and for the mass determination of the binary. In principle, both emission lines from the heated front-side and absorption lines from the photosphere, can be used for the mass determination, if the observed radial velocity amplitude is corrected from center-of-light to center-of-mass velocity. The crucial role of irradiation in this respect was firstly recognized in the prototypical system AM Her by Davey & Smith (1992).

Fig. 13 shows the results of combined He I $\lambda 4686$ and Na I $\lambda 8183/8194$ Doppler tomography of the long-period polars QQ Vul and V1309 Ori ($P_{\text{orb}} = 3.71$ h and 7.98 h, respectively) observed in high accretion states and of the short-period polar HU Aqr ($P_{\text{orb}} = 2.08$ h) which was observed in an intermediate to low accretion state (Catalán et al. 1999, Schwope et al. 2000, Staude et al. 2000, Steeghs et al. 2000). In the high accretion state of HU Aqr the Na I $\lambda 8183/8194$ absorption lines cannot be recognized due to their relative weakness. All four systems (the three shown in Fig. 13 and AM Her) show similar structures on the Roche surface of the secondary star with emission

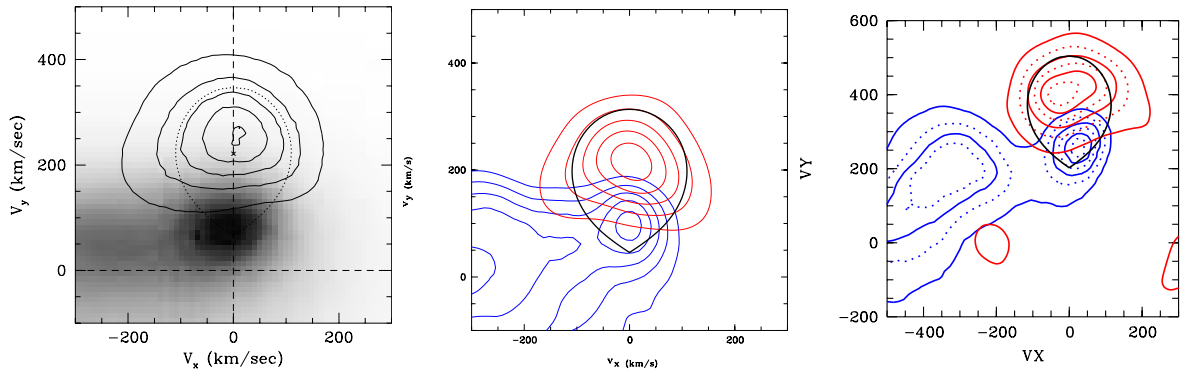


Abbildung 13: Combined Doppler maps of Na I λ 8183/8194 absorption lines and He II λ 4686 emission lines of the AM Herculis systems QQ Vul, V1309 Ori, and HU Aqr. The size of the Roche lobe of the donor star is drawn in each panel for the most likely mass ratio Q (left panel adapted from Schwope et al. 2000, middle panel from Staude et al. 2000 (submitted to A&A), right panel from Steeghs et al. 2000 (in preparation)).

and absorption lines originating at mutually excluding sites.

The He II λ 4686 emission lines originate on the X-ray irradiated front-side of the donor star. A detailed comparison of the emission line radial velocities of these narrow emission lines in QQ Vul shows that the lines of different atomic species originate at different level (i.e. radial velocity) in the atmosphere of the secondary. The higher ionization species like He II λ 4686 originate at the highest atmospheric levels, i.e. closest to the center of mass (Catalán et al. 1999, Schwope et al. 2000). Whether this is a common feature of all polars in their high accretion states needs to be investigated in detail.

The absorption lines of Na I λ 8183/8194 originate almost exclusively on the non-irradiated hemispheres of the donor stars away from the white dwarf. Although the luminosity of the irradiating source is higher than that of the exposed star most of the X-ray photons are absorbed in upper atmospheric layers. This is due to the high column density above the photosphere which easily exceeds 10^{24} atoms cm^{-2} and the fact, that polars typically have soft X-ray spectra. As a consequence, an accretion-induced chromosphere is formed. Only the hard X-ray photons are able to penetrate down to sub-photospheric layers where their energy is finally deposited (King 1989). Hence, the depletion of absorption lines from the region around the L_1 point, the appearance of the donors as half stars in Doppler space, indirectly confirms the presence of a sufficiently powerful hard X-ray source at the time of the optical observation. This is true for all three systems presented here although HU Aqr was encountered in a low accretion state.

Only at further reduced accretion rate (the lowest observed rates are of the order 10^{-13} M_{\odot}/yr the typical rate of a polar below the period gap is about 10^{-10} M_{\odot}/yr) the Na I λ 8183/8194 radial velocity curve become apparently unaffected by irradiation (see Schwope et al. 1993 for the case of MR Ser, Schwope et al. 1997 for the case of UZ For).

The emission line Doppler maps of HU Aqr (Figs. 6 and 13) show the shielding effect of the accretion curtain on the trailing side of the secondary star. One could expect a corresponding mirrored asymmetry in the Na I λ 8183/8194 map. This is not evident in the observed map (Fig. 13), probably due to the low signal-to-noise ratio of the input data. The Na I λ 8183/8194 map of AM Her (Davey & Smith 1992, see also Southwell et al. 1995, Davey & Smith 1996), clearly shows such an asymmetry, and it appears likely that this is also related to the shielding effect of an accretion curtain.

There are no model calculations available in the literature which may be applied directly to the X-ray irradiated hemisphere of a donor star in a polar. The physical scenario is similar to the HZ Her/Her X-1 system where several models with different level of sophistication were developed (e.g., London et al. 1981) but the type of the irradiated star and of the irradiating source are clearly different in the two types of stars. Brett & Smith (1993) published a first model for irradiated donors in CVs, but neither X-ray irradiation, they used a 17000 K white dwarf atmosphere, nor non-LTE radiative transport were taken into account.

The formation and structure of an irradiation-induced quasi-chromosphere and the structure of a hard X-ray heated photosphere can be addressed only by proper numerical modeling of an X-ray irradiated atmosphere. Even then the problem will be solved only under strong simplification, e.g. neglect of meridional heating. In order to compare it with observations on the other hand, it needs geometric sophistication by e.g. proper treatment of shielding by an accretion curtain. A practical application of such computations would be a proper K -correction scheme for the correction of measured radial velocity amplitudes to give the true orbital velocity. The presently

applied schemes (e.g. Southwell et al. 1995, Schwobe et al. 1993) simply assume a strict black/white dichotomy between the irradiated and non-irradiated parts of the star.

Observationally, imaging of the donor stars is a challenging and rewarding task. The maps shown in Fig. 13 are based on data obtained at 4m-class telescopes under non-optimal observing conditions. With present-day instrumentation it will be possible, as model computations have shown, to determine the size of the Roche lobe of the donor star in a long-period polar in Doppler space with better than 10% accuracy by straight application of Doppler tomography. The next step then is to search for structures like star spots in these maps. Up to now star spot imaging was possible only for rapidly rotating single giant stars or those in RS CVn binaries (see e.g. Strassmeier et al. 1999 and references therein). The rotation velocities in CVs are much (factor 10) higher than in the giant stars investigated so far for star spot activity. This means that lower spectral resolution observations of CVs may yield similarly good resolution of the surface of the star. Even though they are much fainter than the giant stars mapped so far, the large light collecting area of the now operational 8m-telescopes will allow star spot imaging for donor stars in CVs. This way a new observational window will be opened in order to address the question of magnetic activity at the bottom of the main sequence.

12 The hot accretion spot on the white dwarf

The accretion spots on the white dwarfs near the polar regions are the sources of emission from the infra-red to the X-ray spectral range. The hot accretion plasma, $kT \sim 10$ keV, cools via hard X-ray bremsstrahlung and cyclotron radiation. The latter is dominant in the infrared and at optical wavelengths. The X-ray spectrum is usually described with two components, the hard component of an optically thin cooling plasma and a soft component from the accretion-heated atmosphere with typical temperature $kT \sim 25$ eV. The soft component typically carries much more flux than the hard component, a phenomenon referred to as soft X-ray puzzle of AM Her stars and explained either in terms of particle or blob heating of the atmosphere instead of radiative heating by the cooling plasma (Kuijpers & Pringle 1982).

Heating of the photosphere either from above by irradiation or below by energy deposited below the photosphere leads to an extended region around the accretion spot with enhanced temperature. These regions with temperatures somewhere between 10^4 K and some 10^5 K, i.e. the temperatures of the photosphere and the X-ray emitting accretion spot, are dominating the ultraviolet spectral range.

The rich phenomenology offers, in principle, a wide field for the application of indirect imaging methods. The light curves in the different spectral ranges are markedly modulated by eclipses (by the companion star) and self-eclipses (by the white dwarf itself) and also by anisotropic emission. However, the following complications may arise if optical and X-ray light curves of radiation sources originating from the hot accretion spot are used for a mapping experiment:

1. The hot accretion region which emits X-ray and optical cyclotron radiation has vertical and lateral extent. Proper disentangling of the geometry is possible only if the latitude of the accretion spot can be reliably determined and if the lateral extent can be fixed. This means that only a high-inclination eclipsing system is promising for spot mapping.
2. The dominant soft X-ray component is subject to pronounced absorption in the binary system and in the very vicinity of the emission region. This is a serious constraint, it means that the visibility function is not only determined by the geometry of the emission region.
3. Cyclotron emission is angular- and frequency-dependent and changes from optically thick at long wavelengths to optically thin at short wavelengths with a transition region of badly determined plasma parameters. In addition, the observed cyclotron spectrum is always a superposition of high- and low-temperature regions with different spectral characteristics.
4. X-ray emission is highly variable on short (seconds to minutes) time-scales. A variable source of emission will inevitably produce spurious features in a brightness map, because a sudden brightness increase will be interpreted by the mapping algorithm as due to a spot of emission which just rotates into view. The only way to reduce the effect of variability is the use of data which were averaged over several orbital cycles.

The first mapping experiment of this kind, an inversion of optical and soft X-ray light curves of ST LMi, was presented by Cropper & Horne (1994). They were facing all the difficulties mentioned but it was not possible to solve them at that time. They assumed a completely flat spot of emission for both types of radiation. ST LMi is not eclipsing, but the accretion region undergoes self-eclipses by the white dwarf. The emission spot found by them is arc-shaped with a core at one extremity in the X-ray map, while the optical map was closely coincident with some additional structure. The under-constrained problem of inverting the light curve leads to artifacts in the map, faint arms stretching north-east and north-west from the main accretion region. These follow the stellar limb as seen at the phases of ingress and egress of the accretion region. Also, an apparent (?) double spot emerges as a consequence of a shoulder in the light curve. Whether such a structure is real or due to internal absorption/extra emission from a raised mound (Sirk & Howell 1998) remains open as long as no extra constraints are applicable.

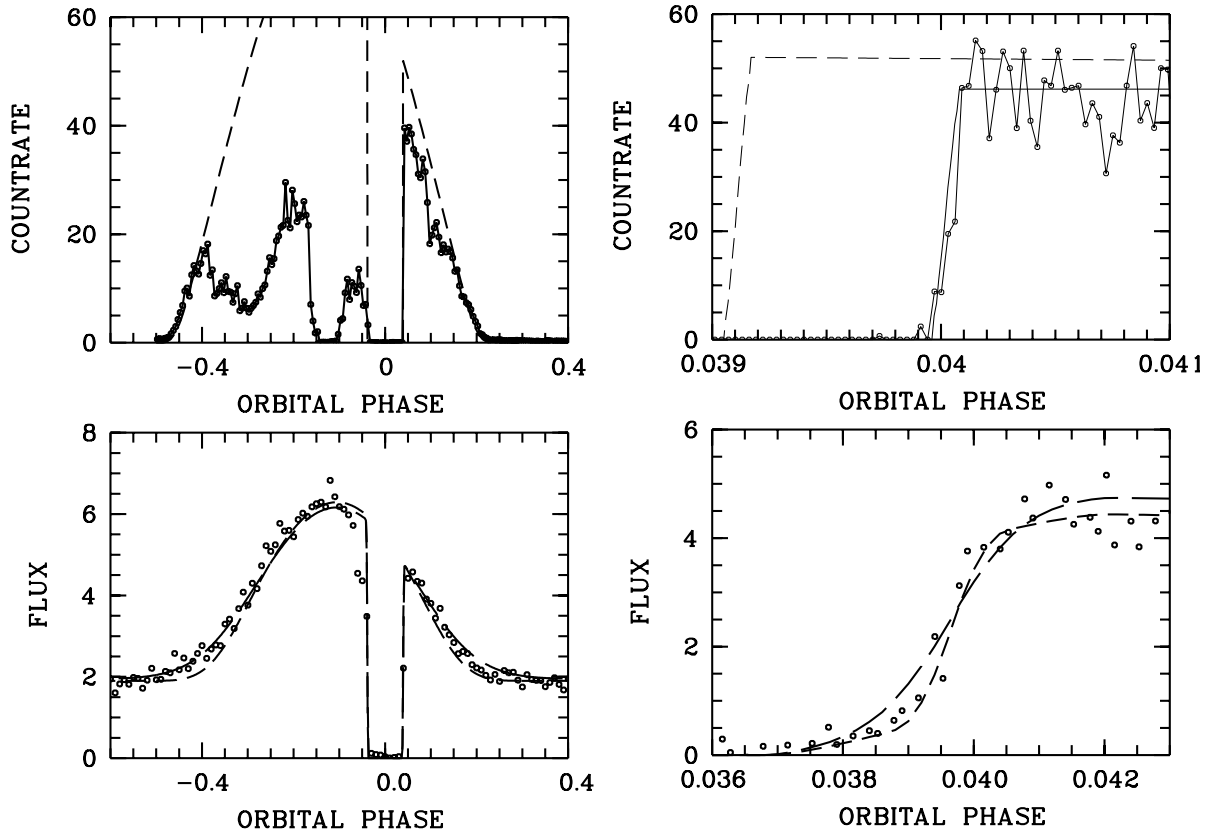


Abbildung 14: High-state X-ray (ROSAT) and low-state ultraviolet (HST/FOS) light curves of HU Aqr together with synthetic light curve. Shown are light curves with full phase coverage and sections centered on eclipse egress.

The inversion process is, at least in principle, much better constrained by a true eclipse. The unique system HU Aqr, shows both eclipses and self-eclipses. On the other hand, optical and X-ray light curves (see Figs. 11 and 14) in the high accretion state are strongly influenced by cyclotron beaming and intrinsic absorption which makes a successful mapping experiment almost impossible. Fig. 14 therefore compares only the results of a forward computation assuming a flat spot in one case and a raised spot in a second case. Eclipse egress, which is contrary to eclipse ingress not or only marginally affected by intrinsic absorption, lasts only 1.3 sec, which means that the accretion spot has an azimuthal extent smaller than $\sim 4^\circ$. A fit to the light curve assuming a flat spot at a high northern co-latitude of only 9° gives a satisfactory fit to the wings of the bright phase, but could be finally excluded due to an imperfect phase match between center of bright phase and true phase zero (fit shown with with dashed line). A spot with vertical extent of about $0.015 R_{\text{wd}}$ at co-latitude 31° and same azimuth of 46° (solid line) gives the same fit to overall light curve than the flat spot model, but places the eclipse at the correct phase.

Most of the problems one encounters when optical and X-ray light curves are inverted can be overcome by inverting ultraviolet light curves. Ultraviolet radiation can reasonably be assumed to originate from a flat extended region, i.e. without vertical extent, it is not or only negligible affected by short-time variability, its spectral composition and angular characteristic is reasonably well understood by stellar atmosphere models. The problem then is to collect appropriate input data. There are two systems which received sufficient coverage by HST thus allowing a kind of mapping experiment to be performed, AM Her and HU Aqr (Gänsicke et al. 1998, Schwöpe et al. in preparation). AM Her was observed in both low and high states by IUE and HST (Gänsicke et al. 1995, Gänsicke et al. 1998). The geometry of AM Her is similar to that of ST LMi with no eclipse, but a self-eclipse of the main accretion region. So far, HST-data were not mapped by an objective inversion method, but by a parameter fitting approach with optimization being achieved by a genetic algorithm (Gänsicke et al. 1998).

The method of Gänsicke assumes a flat circular spot with some form of temperature decrease from a central peak down to the undisturbed photosphere. The parameters to be optimized are the orbital inclination, the location of the spot, the size of the spot, the distance to and the radius of the white dwarf, the extent of the

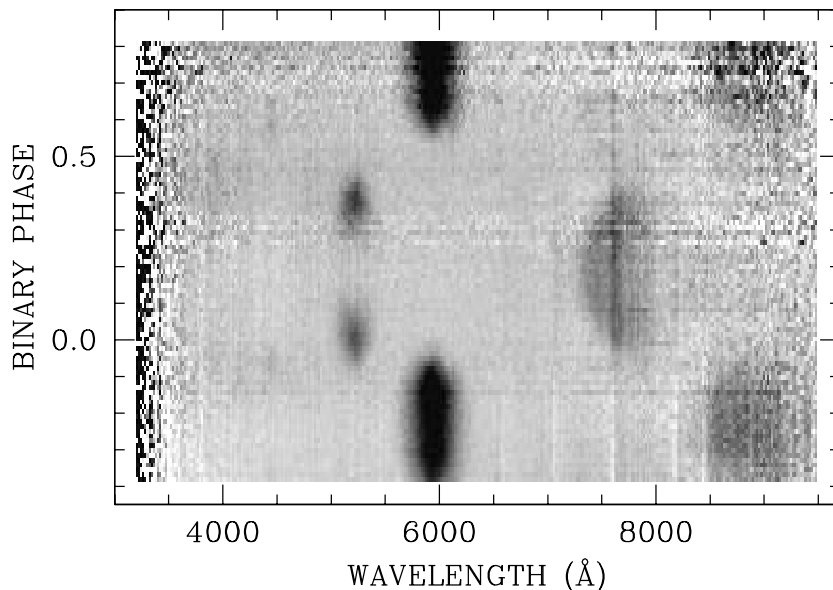


Abbildung 15: Trailed low-resolution spectrogram of HS1023+39 showing cyclotron line emission from two accretion spots at ~ 60 MG and ~ 68 MG (Reimers et al. 1999; the data were kindly provided by H.-J. Hagen).

spot, the photospheric and the central peak temperature. The spectral flux at given wavelength for a specific temperature is interpolated between data bank entries for hot, high-gravity, pure hydrogen model spectra.

The best fit using this model for AM Her (HU Aqr, see Fig. 14) predicts a rather large accretion spot of opening angle $\theta \simeq 70^\circ$ with peak temperature $T_c = 47000$ K. However, without the extra constraint of a true eclipse it is possible to trade the opening angle versus the peak temperature. A model with T_c as large as 200000 K with $\theta = 28^\circ$ could not be ruled out. This means that the predictive power of the method applied to a non-eclipsing system is rather limited.

Some preliminary results of our modeling of HU Aqr are shown in Fig. 14 (bottom panels). As for AM Her, the best fit to the HST/FOS continuum data for the whole bright phase excluding the eclipse is a rather large spot with half opening angle $\theta \sim 50^\circ$ and central temperature 34000 K (fit shown with long-dashed lines; the temperature of the undisturbed photosphere was 14000 K). This gives a smooth fit to the wings of the bright phase. It gives a bad fit to the eclipse data, which is much better fitted with peak temperature as high as 80000 K and an opening angle of 22° (the corresponding fit is shown with short-dashed lines, still a preliminary result).

The synoptic view allowed by the unique system HU Aqr illustrates the difficulties one encounters if one tries inversion of the light curve(s) in an objective manner: these are the limited number of photons, the short duration of the critical events, and the uncertain and wavelength-dependent geometry of the emitting region. On the X-ray side some progress will be made in the near future by the XMM-observations of eclipsing polars, on the ultraviolet side no significant observational progress can be expected in the foreseeable future unless some bright, eclipsing system will be newly discovered and thoroughly observed with HST.

Optical data might play a more important rule in the future if one makes full use of the directional characteristics of cyclotron radiation in the modeling process. A first such attempt has been undertaken by Potter et al. (1998, 2000a, 2000b, see also this volume) with the concept of Stokes imaging. Although promising, this attempt suffers so far from the observational side from the use of broadband polarimetry only, and from the modeling side from the neglect of an unpolarized background radiation and the use of homogeneous temperature models only. The active regions emerging from this inversion are rather large, contrary to the expectation that they should similar in size as the X-ray emitting regions.

The next logical step is the use of high-time resolution data with spectral and polarimetric resolution. This kind of data will allow proper modeling of the cyclotron spectrum, which inherently carries temperature and angular information about the emitting plasma and allows, under lucky circumstances, proper treatment of background radiation components. Some early examples of the necessary type of data and modeling were presented for MR Ser and UZ For by Schwope et al. (1993) and Rousseau et al. (1996). These systems showed at low accretion rate in their optical spectra deeply modulated cyclotron harmonics. Meanwhile other systems were discovered with similar properties, a trailed spectrum of one particularly beautiful example, HS1023+3900 (Reimers et al. 1999),

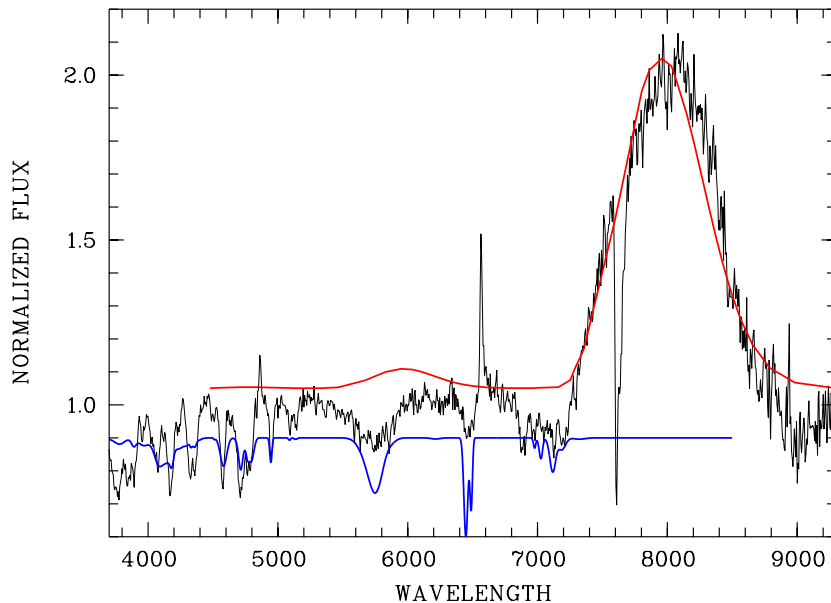


Abbildung 16: Low-resolution normalized spectrum of RBS0206 (1RXS J012851.9–233931) showing a strong cyclotron line in the red ($B_c = 45 \pm 1$ MG) and a photospheric Zeeman spectrum of a mean surface field $B_Z = 36 \pm 1$ MG (Schwope et al. 1999).

is reproduced in Fig. 15. Twin systems with similar cyclotron lines are RBS0206 (Schwope et al. 1999) and HS0922+1333 (Reimers & Hagen 2000). These systems are distinguished from most of the others by completely un-blended cyclotron lines which appear and disappear as the cyclotron emitting plasma becomes self-eclipsed by the white dwarf. Similarly to the X-ray light curve of HU Aqr shown above in Fig. 14, a complete disentangling of the geometry is almost impossible without a genuine eclipse by the secondary star, but it seems to be only a matter of time until such a system will be found in the sky. It seems reasonable then to think of physical parameter eclipse mapping (see Vrielmans’s contribution to this volume) of such a system with temperature, field geometry and field strength as physical parameters to be mapped.

13 The structure of the white dwarfs magnetic field

The first Zeeman spectra of AM Her were obtained in a low accretion state and published some 20 years ago (Latham et al. 1981). Since then, photospheric Zeeman lines were detected in about a dozen systems (for a recent review see Wickramasinghe & Ferrario 2000).

Phase-resolved Zeeman spectroscopy of AM Her (Latham et al. 1981; Wickramasinghe & Martin 1985), MR Ser (Schwope et al. 1993), and BL Hyi (Schwope et al. 1995) has provided unambiguous evidence for field distributions which differ from a centered dipole, the usual first approximation. As a second approximation, those field structures were modeled by dipoles which were offset from the center of the star by $0.1\text{--}0.3 R_{\text{wd}}$ along the dipole axis. However, these *ad hoc* models bear ambiguities and are far away from yielding unique solutions. The more appropriate approach is a multi-pole expansion or indirect imaging of the field without any pre-defined underlying morphology. This makes phase-resolved Zeeman spectroscopy/spectropolarimetry necessary. The targeted system should have a largely uncontaminated Zeeman spectrum of the white dwarf. This is not easy to achieve, since accretion-induced radiation components are usually prevalent in polars. Even in low accretion states, remaining cyclotron emission and recombination radiation from the stream are often not negligible. An important role for such a mapping experiment might play the systems with persistent low accretion rate (HS1023, HS0922, RBS0206) introduced in the previous section. One template spectrum of RBS0206 showing a rather clean separation of the photospheric Zeeman spectrum and the accretion-induced cyclotron spectrum is reproduced in Fig. 16.

By application of an indirect imaging technique to a series of phase-resolved spectra the underlying field structure can be uncovered. A corresponding feasibility study for magnetic white dwarf stars was presented by Donati et al. (1994). At that time suitable data for single white dwarfs were missing. The main problem with these stars is the often unknown rotational period or, if known, the inappropriate high field strength. High-field stars with $B > 50$ MG, are presently inappropriate, because current Zeeman models cannot properly reflect the

continuum polarization. On the other hand, large fields provide the largest Zeeman split and are thus most sensitive to variations of the field strength.

At least as long as continuum polarization is not properly addressed in Zeeman model spectra, the magnetic white dwarfs in polars form an important sample for such an indirect imaging experiment. Most of the magnetic white dwarfs in polars have a field strength below 50 MG (see the recent compilation by Wickramasinghe & Ferrario 2000) and all have known rotational periods. The presence of contaminating cyclotron radiation poses an extra difficulty to the method. On the other hand, the presence of one or two cyclotron line systems provides us with a boundary condition for the field strength at one or two particular places on the surface of the white dwarf. An additional complication is accretion heating of the polar cap(s) which has to be taken into account in the inversion process. Hence, a grid in magnetic field strength, orientation, temperature, and perhaps abundance is the minimum prerequisite for a successful mapping experiment which is otherwise technically feasible.

14 Summary

I have reviewed the results of indirect imaging techniques applied to AM Herculis stars or polars. The techniques discussed here are Doppler tomography, accretion stream mapping ASM, accretion spot mapping, and Zeeman imaging of the white dwarf accreting star. Further techniques described in this volume by Dhillon and Potter are Roche tomography and Stokes imaging. Although rather small in number and rather faint in brightness the polars offer a wide field for the application of tomographic and mapping techniques due to their preferred geometry, their handy period, and the multitude of physical processes which lead to radiation of different kind, at different wavelengths, and with fundamentally different properties.

The sites of emission studied here are the accretion stream, the accretion curtain and the irradiated hemisphere of the donor star which become visible in the light of reprocessed atomic line radiation in Doppler tomograms. We have found quasi-ballistic accretion streams which are slightly influenced by the presence of the magnetic field of the white dwarf. We have found in addition in a few systems magnetically controlled streams, which allow the orientation of the magnetic field to be investigated. Our theoretical understanding of Doppler maps needs to be developed in detail taking into account the excitation by the X-ray source and the ionization structure in the stream. Extended emission structures neither resembling a disk or a simple accretion curtain as seen in intermediate polars were uncovered in asynchronously rotating polars. For the time being we can state only, that blue- and red-shifted emission lines are seen simultaneously without being able to sketch a convincing geometry for these systems.

The donor stars became visible, i.e. resolved, in Doppler maps of photospheric absorption lines and the dramatic influence of X-ray irradiation on the structure of their photospheres became obvious. Again, a detailed theoretical understanding of the underlying physics needs to be developed. I'm quite confident that soon the first starspots on a late-type ZAMS (or near-ZAMS) donor star can be made visible by straightforward application of Doppler tomography or its derivative, by Roche tomography. Then the question of magnetic activity at the bottom of the main sequence can be addressed by watching through a new observational window.

Accretion Stream Mapping is found to be a useful technique complementing Doppler tomography in order to derive the brightness map along the accretion stream. Both methods have their short-comes and a substantial step forward can be reached by their combination, Eclipse Doppler Tomography. The necessary input data can be obtained in the era of the giant 8-10m class telescopes.

Mapping experiments of the accretion spot using only self-eclipses by the white dwarf lack uniqueness due to the uncertain geometry. The geometry can in principle be nailed down using in addition true eclipses by the secondary star. Since these are extreme short-lasting events, one is limited by the high degree of variability of the radiation (in X-rays), and the limited number of photons (UV and X-ray range). Some development can be expected from high time-resolved cyclotron spectroscopy in the optical which will eventually allow a physical parameter eclipse mapping of the accretion spot.

Zeeman imaging of the magnetic white dwarf finally will almost definitely be possible in the near future as soon as codes for atmospheric models are fully developed and as an almost uncontaminated Zeeman spectrum is obtained. A small number of low-accretion rate polars suited for this investigation were discovered recently. More will follow, if the present census of polars, which is heavily biased by the optical identification of X-ray counterparts, i.e. biased towards high-accretion rate systems, is enriched by optically selected systems, which may emerge from e.g. variability surveys. Once successful, the Zeeman images of white dwarf stars in polars will shed new light on the field structure of the white dwarfs themselves as well as of their progenitors.

Acknowledgements

I would like to thank Sonja Vrielmann, Danny Steeghs, and Boris Gänsicke, who shared my interest and their codes for exploring the secrets of polars. Special thanks go to Keith Horne and Henk Spruit for providing their Doppler tomography codes. Gary Schmidt, Susanne Friedrich, Ralf Geckeler, Rüdiger Staubert, Gyula Szokoly, Robert

Schwarz, and H.-J. Hagen kindly allowed me to present their data of AR UMa, V1432 Aql, EUVE J1429–38, BY Cam, and HS1023+3900, respectively, in this review. K.-H. Mantel operated the MCCP during three beautiful nights under a clear Calar Alto sky. Without the help of my colleagues at the AIP, Robert Schwarz and Andreas Staude, this study would not have been possible.

This project was supported by the Bundesministerium für Bildung und Forschung through the Deutsches Zentrum für Luft- und Raumfahrt e.V. (DLR) under grant number 50 OR 9706 8. The responsibility for the content of the publication lies with the author.

Literatur

- [1] J. Bailey: ASP Conf. Ser. 85, 10 (1995)
- [2] J. Bailey, M. Cropper: MNRAS 253, 27 (1991)
- [3] A. Bobinger: A&A 357, 1170 (2000)
- [4] A. Bobinger, H. Barwig, H. Fiedler, K.-H. Mantel, D. Simic, S. Wolf: A&A 348, 145 (1999)
- [5] J.M. Brett, R.C. Smith: MNRAS 264, 641 (1993)
- [6] C.G. Campbell, A.D. Schwope: A&A 343, 132 (1999)
- [7] M.S. Catalán, A.D. Schwope, R.C. Smith: MNRAS 310, 123 (1999)
- [8] M. Cropper, K.D. Horne: MNRAS 267, 481 (1994)
- [9] S. Davey, R.C. Smith: MNRAS 257, 476 (1992)
- [10] S. Davey, R.C. Smith: MNRAS 280, 481 (1996)
- [11] M.P. Diaz, J.E. Steiner: A&A 283, 508 (1994a)
- [12] M.P. Diaz, J.E. Steiner: ApJ 425, 252 (1994b)
- [13] Donati, J.-F., N. Achilleos, J.M. Matthews, F. Wesemael: A&A 285, 285 (1994)
- [14] B.T. Gänsicke, D.W. Hoard, K. Beuermann, E.M. Sion, P. Szkody: A&A 338, 933 (1998)
- [15] P.J. Hakala: A&A 296, 164 (1995)
- [16] M.K. Harrop-Allin, P.J. Hakala, M. Cropper: MNRAS 302, 362 (1999a)
- [17] M.K. Harrop-Allin, M. Cropper, P.J. Hakala, C. Hellier, T. Ramseyer: MNRAS 308, 807 (1999b)
- [18] C. Heerlein, K. Horne, A.D. Schwope: MNRAS 304, 145 (1999)
- [19] C. Hellier: ApJ 519, 324 (1999)
- [20] R.H. Kaitchuck, E.M. Schlegel, R.K. Honeycutt, et al.: ApJS 93, 519 (1994)
- [21] A.R. King: MNRAS 241, 365 (1989)
- [22] J. Kube, B.T. Gänsicke, K. Beuermann: A&A 356, 490 (2000)
- [23] J. Kuijpers, J.E. Pringle: A&A 114, L4 (1982)
- [24] D.W. Latham, J. Liebert, J.E.: ApJ 246, 919 (1981)
- [25] R. London, R. McCray, L.H. Auer: ApJ 243, 970 (1981)
- [26] S.B. Potter, P.J. Hakala, M. Cropper: MNRAS 297, 1261 (1998)
- [27] S.B. Potter: MNRAS 314, 672 (2000a)
- [28] S.B. Potter, M. Cropper, P.J. Hakala: MNRAS 315, 423 (2000b)
- [29] D. Reimers, H.-J. Hagen: A&A 358, L45 (2000)
- [30] D. Reimers, H.-J. Hagen, U. Hopp: A&A 343, 157 (1999)
- [31] T. Rousseau, A. Fischer, K. Beuermann, U. Woelk: A&A 310, 526 (1996)
- [32] G.D. Schmidt, P. Szkody, P.S. Smith, et al.: ApJ 473, 483 (1996)
- [33] G.D. Schmidt, D.W. Hoard, P. Szkody, F. Melia, R.K. Honeycutt, R.M. Wagner: ApJ 525, 407 (1999)
- [34] A.D. Schwope, K. Beuermann, S. Jordan: A&A 301, 447 (1990)
- [35] A.D. Schwope, K. Beuermann, H.-C. Thomas: A&A 230, 120 (1990)
- [36] A.D. Schwope, S. Mengel, K. Beuermann: A&A 320, 181 (1997)
- [37] A.D. Schwope, K.-H. Mantel, K. Horne: A&A 319, 894 (1997)

- [38] A.D. Schwope, R. Schwarz, J. Greiner: *A&A* 348, 861 (1999)
- [39] A.D. Schwope, M.S. Catalán, K. Beuermann, et al.: *MNRAS* 313, 533 (2000)
- [40] A.D. Schwope, K. Beuermann, S. Jordan, H.-C. Thomas: *A&A* 278, 487 (1993)
- [41] A.D. Schwope, R. Schwarz, A. Staude, C. Heerlein, K. Horne, D. Steeghs: *ASP Conf. Ser.* 157, 71 (1999)
- [42] A.W. Shafter, K. Reinsch, K. Beuermann, et al.: *ApJ* 443, 319 (1995)
- [43] K.B. Sohl, G. Wynn: *ASP Conf. Ser.*, 157, 87 (1999)
- [44] K.A. Southwell, M.D. Still, R.C. Smith, J.S. Martin: *A&A* 302, 90 (1995)
- [45] H. Spruit: *astro-ph/9806141* (1998)
- [46] D. Steeghs, K. Horne, T.R. Marsh, J.F. Donati: *MNRAS* 281, 626 (1996)
- [47] K.G. Strassmeier, S. Lupinek, R.C. Dempsey, J.B. Rice: *A&A* 347, 212 (1999)
- [48] S. Vrielmann, A.D. Schwope: *MNRAS*, in press (2000)
- [49] F.K. Walter, S.J. Wolk, N.R. Adams: *ApJ* 440, 834 (1995)
- [50] D.T. Wickramasinghe, L. Ferrario: *PASP* 112, 873 (2000)
- [51] D.T. Wickramasinghe, B. Martin: *MNRAS* 212, 353 (1985)